

Distribution Agreement

In presenting this thesis or dissertation as a partial fulfillment of the requirements for an advanced degree from Emory University, I hereby grant to Emory University and its agents the non-exclusive license to archive, make accessible, and display my thesis or dissertation in whole or in part in all forms of media, now or hereafter known, including display on the world wide web. I understand that I may select some access restrictions as part of the online submission of this thesis or dissertation. I retain all ownership rights to the copyright of the thesis or dissertation. I also retain the right to use in future works (such as articles or books) all or part of this thesis or dissertation.

Signature:

Fuchang Yin

Date

Simulations of Lipid Sorting Effects near Transmembrane Peptide

By

Fuchang Yin
Doctor of Philosophy

Department of Chemistry

Dr. James T. Kindt
Advisor

Dr. Joel M. Bowman
Committee Member

Dr. Stefan Lutz
Committee Member

Accepted:

Lisa A. Tedesco, Ph.D.
Dean of the James T. Laney School of Graduate Studies

Date

Simulations of Lipid Sorting Effects near Transmembrane Peptide

By

Fuchang Yin
M.Sc. Mississippi State University, 2004

Advisor: James T. Kindt, Ph.D.

An Abstract of
A dissertation submitted to the Faculty of the
James T. Laney School of Graduate School of Emory University
in partial fulfillment of the requirements for the degree of
Doctor of Philosophy
in Chemistry
2011

Abstract

Simulations of Lipid Sorting Effects near Transmembrane Peptide

By Fuchang Yin

A biological membrane is a dynamic structure composed of a diverse set of proteins and other biomolecules embedded in a lipid bilayer containing many different types of lipid. The diversity of lipids and proteins raises the question of whether lipids of different types are distributed randomly in the membrane, or associate preferentially with particular proteins. The hydrophobic matching concept, which suggests that peptides are most stable when inserted in bilayers whose hydrophobic thickness matches the peptide's hydrophobic span, is considered one of the most important factors in the lipid-peptide interplay. In bilayers containing lipids with different hydrophobic tail lengths, the hydrophobic matching effect would in general sort lipids resulting in enrichment of the best hydrophobic matched lipid type near peptide. Various experimental methods have been applied to measure this sorting, in model bilayer systems with just a few components, but face many difficulties in interpretation due to the disorder and fluidity of the bilayer. Molecular dynamics (MD) computer simulation methods have been successfully applied to study lipid bilayers with one lipid type, and could usefully complement these experiments. However, this conventional method is not efficient enough to study systems containing more than one lipid type, since slow lipid diffusion rate will require long molecular dynamics simulations, exceeding readily available computational capacities, to adequately sample the distribution states of the lipid mixtures. In this study, a hybrid Monte Carlo-molecular dynamics (MC-MD) approach, which uses mutation moves to interchange lipid types throughout the system within the semi-grand canonical ensemble, is used to overcome the simulation difficulty of lipid diffusion. Pairs of saturated phosphatidylcholine lipids, distearoylphosphatidylcholine (DSPC), dimyristoylphosphatidylcholine (DMPC), and didecanoylphosphatidylcholine (DDPC), differing by four carbons in the lengths of their acyl tails, are selected to form two-component lipid bilayers. The lipid redistribution in mixed lipid bilayer containing DSPC-DMPC or DMPC-DDPC, induced by an embedded transmembrane peptide is investigated in using MC-MD simulation. Firstly, the alpha helical Neu_{TM35} peptide is chosen, in which position restraints are applied to the peptide backbone to avoid helix unraveling. Enrichment of DMPC is found in the DMPC-DDPC system. Secondly, study of WALP23/KALP23 peptide from the more stable alpha helical peptide family suggests a strong peptide tilt in the lipid bilayer to accommodate hydrophobic matching instead of changing the bilayer thickness. Thirdly, strong thickness perturbations but weak sorting of lipids is observed in gramicidin A transmembrane ion channel, suggesting hour-glass shape and strong tilt of the peptide would account for reduction of lipid sorting. Finally, a large cylindrical beta barrel OmpA peptide is investigated. Both hydrophobic matching and hydrophobic sorting effects are evident, and the difference in degree of sorting for DMPC-DDPC and DSPC-DMPC systems validates the quadratic relationship of free energy change and hydrophobic mismatch early predicted by theory. The atomistic simulation result also suggests that Coarse Grained model can be used in studying hydrophobic sorting by MD simulations.

Simulations of Lipid Sorting Effects near Transmembrane Peptide

By

Fuchang Yin
M.Sc. Mississippi State University, 2004

Advisor: James T. Kindt, Ph.D.

A dissertation submitted to the Faculty of the
James T. Laney School of Graduate School of Emory University
in partial fulfillment of the requirements for the degree of
Doctor of Philosophy
in Chemistry
2011

Acknowledgments

First, I would like to thank the National Science Foundation, the Camille and Henry Dreyfus Foundation, and James T. Laney School of Graduate School of Emory University for financial support.

I would like to express my special thanks to my Ph.D. advisor, Professor James T. Kindt, for his valuable advice, patience and enthusiasm throughout my graduate school. Every time I encounter problems and seek advisement, he has been very helpful and supportive. The solutions he gave to me are not only limited to the question itself, but also extend to in-depth knowledge related to the problem I have encountered, which makes me attracted by many interesting areas in science and technology besides my primary research projects. In addition to pointing out the right directions for my interest, Dr. Kindt provided me a very relaxed environment to grow. I learned new things from making mistakes and became mature after training and education obtained from him. His wonderful guidance made me more precise in science, more efficient in study, more confident in work, which will be a treasure for my whole life.

I would also like to thank my committee members, Professors Joel Bowman and Stefan Lutz for their useful guidance and advice over the past five years.

I would like to dedicate my today's achievements to my dear parents, Minghui Yin and Lanning Liu, my wife Jin Wang and my daughter Iris Siqi Yin. This dissertation would

not have been possible without their unlimited love and support to encourage me throughout these years.

I would like to specially thank Dr. Djamaladdin (Jamal) Musaev and Dr. Alex Kaledin who provided wonderful technical support in my Ph.D. research at the Cherry L. Emerson Center for Scientific Computation.

My final acknowledgement goes to the Kindt group members, Yong Jiang, Xinjiang Lü, Hao Wang, Patrick S. Coppock, Ana West. It is such an unforgettable time for me being in this lab for five years.

Table of Contents

List of Tables	vii
List of Figures	viii
References to Previously Published Work	x
1. Introduction	1
1.1. Background and Overview	1
1.2. Hybrid Molecular Dynamics and Monte-Carlo Methods	12
1.3. Outline of Thesis	13
2. Atomistic Simulation of Hydrophobic Matching Effects on Lipid Distribution	
Near a Monomer of Neu/Erb2 Transmembrane Domain	17
2.1. Abstract	17
2.2. Introduction	18
2.3. Method	20
2.3.1. Molecular Dynamics and Hybrid MC-MD Setup	20
2.3.2. Configuration Construction	21
2.3.3. Positional Constraint of Peptide in Simulation	22
2.3.4. Equilibration	23
2.3.5. Simulations	24
2.4. Results and Discussion	26
2.5. Conclusions	36

3. Hydrophobic Sorting Effect Studies with Engineered WALP/KALP	
Alpha Helices	38
3.1. Introduction	38
3.2. Method	39
3.3. Results and Discussion	40
3.4. Conclusions	42
4. Atomistic Simulation of Hydrophobic Sorting Effects Near Beta Helix: the Gramicidin A Transmembrane Ion Channel	43
4.1. Abstract	43
4.2. Introduction	43
4.3. Method	47
4.3.1. Simulation Configuration	47
4.3.2. System Construction	48
4.4. Results and Discussion	50
4.4.1. Hydrophobic Matching	50
4.4.2. Hydrophobic Sorting	54
4.4.3. Peptide Tilt	57
4.5. Conclusions	58
5. Simulations of Lipid Sorting Effects near Beta Barrel Peptide with Atomistic Model and Coarse Grained Model	60
5.1. Abstract	60
5.2. Introduction	60
5.3. Method	64

5.3.1. Coarse-grained model simulations.....	64
5.3.2. Atomistic model simulations	65
5.3.3. Mixed Monte Carlo/MD simulations	67
5.3.4. Thickness Analysis.....	67
5.4. Results and Discussion.....	68
5.4.1. Coarsed Grained System.....	68
5.4.2. Atomistic System.....	72
5.5. Conclusions.....	84
References.....	86

List of Tables

2.1	Average lipid compositions at different starting configurations and activity ratios	24
3.1	Simulated temperatures of systems mixed with peptide and lipids	40
4.1	Average lipid compositions at different starting configurations and activity ratios in binary lipid mixtures.....	51
5.1	Bilayer thickness of the peptide embedded coarse grained systems.....	70
5.2	Average lipid compositions at in starting configurations and activity ratios.....	74

List of Figures

1.1	Schematic illustration of hydrophobic matching of an integral membrane protein	4
1.2	Schematic illustration of a lipid bilayer with embedded proteins and two different lipid types	9
2.1	Lipid bilayer composition change against time	25
2.2	Radial distribution of DMPC-DDPC system composition and bilayer thickness	26
2.3	Top and cross-sectional views of snapshots of final simulation structures of Neu _{TM35} peptide in mixed DMPC-DDPC bilayers	28
2.4	Lateral atomistic distribution of DMPC over lipids	29
2.5	Scatter plot of lipid phosphorus atom positions for lipids near the peptide in upper and lower mono layer for simulation with 55.8% DMPC, 44.2% DDPC	30
2.6	Radial distribution of DMPC-DSPC system composition and bilayer thickness	32
2.7	C-H bond order parameters for methylene and methyl groups of lipid acyl tails by position in the tail, averaged over all protons on both tails	33
2.8	C-H bond order parameter differences between system with peptide and without peptide	34
3.1	Snapshot at 20 ns for WALP23-NH2 peptide in DDPC bilayer at 330K	41
3.2	Radial distribution of DMPC in the DMPC-DDPC/WALP23-NH2 system	41
4.1	Lipid bilayer thickness as radial distance to the center of mass of peptide	51

4.2	Longer lipid composition percentage as radial distance to the center of mass of peptide	53
4.3	Radial distribution of lipid head groups and lipid tail groups from center of peptide	56
4.4	Gramicidin A dimer in hourglass shape.....	56
4.5	GCA tilt angle in the second part of MCMD.....	58
5.1	Lipid bilayer thickness in Coarse-Grained simulations.....	70
5.2	Lipid identity radial distribution of 1000-2000 ns Coarse-Grained simulations	71
5.3	Snapshots of OmpA in crystal state and embedded in bilayer	72
5.4	Hydrophobic matching of lipids as function of radial distance from peptide.....	74
5.5	Lipid radial distribution for DMPC-DDPC and DSPC-DMPC mixture	77
5.6	Mean excess number of longer tail lipid to the control average versus radial distance from the center of peptide.....	80
5.7	Lipid lateral distribution in the mixed lipid bilayer with embedded peptide.....	81
5.8	Average C-H bond order parameter profile	82

References to Previously Published Work

1. Jason de Joannis, Yong Jiang, Fuchang Yin and James T. Kindt, "Equilibrium distributions of dipalmitoyl phosphatidylcholine and dilauroyl phosphatidylcholine in a mixed lipid bilayer: Atomistic semigrand canonical ensemble simulations." *Journal of Physical Chemistry B*, **2006**, *110*, 25875.
2. Hao Wang, Jason de Joannis, Yong Jiang, Jeffrey C. Gaulding, Birgit Albrecht, Fuchang Yin, Kunal Khanna, and James T. Kindt. "Bilayer Edge and Curvature Effects on Partitioning of Lipids by Tail Length: Atomistic Simulations." *Biophysical Journal*, **2008**, *95*, 2647.
3. David C. Turner, Fuchang Yin, James T. Kindt, and Hailing Zhang, "Molecular dynamics simulations of glycocholate-oleic acid mixed micelle assembly." *Langmuir*, **2010**, *26*, 4687.
4. Fuchang Yin and James T. Kindt, "Atomistic Simulation of Hydrophobic Matching Effects on Lipid Composition near a Helical Peptide Embedded in Mixed-Lipid Bilayers." *Journal of Physical Chemistry B*, **2010**, *114*, 8076.
5. Jason de Joannis, Patrick S. Coppock, Fuchang Yin, Makoto Mori, Absalom Zamorano, and James T. Kindt. "Atomistic simulation of cholesterol effects on miscibility of saturated and unsaturated phospholipids: implications for liquid-ordered/liquid-disordered phase coexistence." *Journal of the American Chemical Society*, **2011**, *133*, 3625.

1 Introduction

1.1 Background and overview

A biological membrane is an enclosing or separating membrane that separates different compartments in the cell. It typically serves as a selective barrier due to its selectively permeable structure, by which a cell can maintain an environment suitable for biological functions that differs from its surroundings¹. Therefore, biological membrane has been identified as one of the most important areas in biological studies. There has long been an interest in basic structural and dynamical aspects of biological membranes. In 1972, Singer and Nicolson² proposed the fluid mosaic model of biological membranes, and this model has been a central paradigm in membrane science. In this model, biological membranes are considered to consist of two components: a lipid bilayer possessing a certain degree of fluidity, and various membrane components, such as cholesterol, peptides, and proteins which are anchored on or embedded in the lipid bilayer. The overall random appearance of this lipid-protein fluid composite made the membrane look like a mosaic. A key property of this model is an extreme degree of fluidity, as the protein molecules are completely free to translate laterally in the lipid bilayer. Continued research has revealed some limitations of this model, such as inadequacy of depicting the bilayer as a virtually naked structure³. Refinements of the fluid mosaic model have been suggested from time to time. In 1977, Israelachvili⁴ proposed a refined fluid-mosaic model in which membrane distortion, pore formation and some degree of heterogeneity are incorporated. A number of theoretical calculations⁵⁻⁹ predicts membrane

heterogeneity and direct¹⁰ and indirect¹¹⁻¹² experimental measurements have suggested that membrane heterogeneity widely exists.

The heterogeneity of membrane is mostly observed in the presence of integrated proteins, which have one or several segments spanning across lipid bilayers. As the function of membrane proteins as well as physical properties of the membrane are regulated by the protein/lipid interactions, extensive and systematic studies of these interactions have become an important area of research. A number of studies have suggested that cell membranes show compositional asymmetric distributions of various components both laterally in the plane of the membrane and between the two sides of the bilayer¹³⁻¹⁸. This arrangement plays an important role in the sorting and self-assembly of proteins and their clustering into high-order oligomers¹⁹⁻²⁰. Because of the heterogeneity of membrane, proteins may partition into different lipid domains, forming functional complexes at specific locations. The lateral distribution of protein and lipid is very important in various cellular processes, such as membrane fusion²¹⁻²², protein trafficking²³, and signal transduction²⁴⁻²⁶. Though the molecular structures of lipids and integral proteins are well characterized, the intermolecular interactions between them that determine the lateral organization remain poorly understood. The incredible complexity of biomembranes has prompted researchers to use experiments on simpler bilayer-based model systems to explore the fundamentals of these interactions. Even so, due to the amorphous structure of the bilayer, experimental characterization of lateral organization in biological membrane under nanoscale remains challenging. Molecular simulation has been

extremely useful in the studies of bilayers, because instead of measuring ensemble-averaged properties by experiments, more detailed structural properties can be obtained.

The integration of transmembrane proteins in the lipid bilayer is one of the most critical features of biomembrane configuration. Integral membrane proteins are characterized by one or more transmembrane segments, consisting primarily of hydrophobic amino acid residues, traversing the hydrophobic interior of lipid bilayers. It is obvious that the maximum exposure of the protein hydrophobic segments to the bilayer hydrophobic interior formed by lipid acyl chains is energetically favorable. In 1984, Mouritsen and Bloom proposed a thermodynamic model for describing lipid-protein interactions in membranes²⁷. In this theoretical model, the mixture of lipids and embedded protein/peptide are characterized as an elastic “mattress” entity, consisting of spring-like protein surrounded by lipids which also have spring-like acyl tails. Based on this model, the hydrophobic matching hypothesis has been proposed to explain the perturbations of the bilayer or protein structure upon protein insertion in this model, and developed further in later studies²⁸⁻³⁰. The hydrophobic matching hypothesis supposes that when the hydrophobic thickness (i.e., lipid bilayer acyl-chain thickness) of the lipid bilayer is not equal to the dimension of the hydrophobic transmembrane domain, then the bilayer, the protein, or both will adapt to promote full hydrophobic solvation of transmembrane domain.

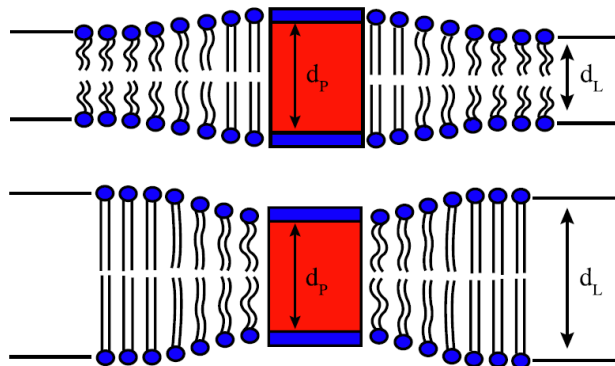


Figure 1.1. Schematic illustration of hydrophobic matching of an integral membrane protein that is embedded in a thin (top) and a thick (bottom) lipid bilayer. Adapted from ref. 29, initially illustrated in ref. 30.

As illustrated in Figure 1.1, the hydrophobic mismatch²⁹⁻³¹ is quantitatively defined as the distance difference between the hydrophobic length of the protein transmembrane segment, d_p , and the hydrophobic thickness of lipid bilayer, d_L .

$$\text{hydrophobic mismatch} = |d_p - d_L| \quad (\text{equation 1.1})$$

Positive mismatch refers to the situation that d_L is greater than d_p and the thickness of lipid bilayer near the protein will increase to accommodate the protein membrane spanning area. Negative mismatch, in contrast, refers to the situation that a local bilayer compression along the bilayer norm would occur. A simplest model containing one transmembrane peptide constrained to be perpendicular to a bilayer with an excess of lipids demonstrates that the free energy of the protein integral system can be expressed³¹ in terms of mismatch as

$$G = G^0 + k \left(\frac{\rho_p}{\pi \xi_L} + 1 \right) (d_p - d_L)^2 \quad (\text{equation 1.2})$$

where G^0 is the free energy of the unperturbed membrane and k is a phenomenological constant related to the compressibility modulus of bilayer area. The term ζ_L is the persistence length of the lipid-bilayer fluctuations, which is assumed to be approximately proportional to the decay length of the protein perturbation. The term ρ_p is the circumference of the protein, which is assumed to have a cylindrical shape. According to this theory, the excess free energy derived from elastic distortion of lipid near the protein is proportional to the square of hydrophobic mismatch and also increases with the thickness of the transmembrane segment. As indicated by the mattress model, the hydrophobic mismatch could result in rearrangement of protein transmembrane segments and lipids, which may explain a wide variety of biophysical phenomena of membranes³⁰⁻³². To a first approximation, one expects that transmembrane segments with similar d_p to be attracted to experience an effective attraction, as each would favor the locally thickened or thinned region surrounding the other.

The structural adaptation of a protein/lipid system to hydrophobic mismatch can take several forms to prevent or reduce exposure of hydrophobic residue to the hydrated lipid bilayer headgroup region and the aqueous phase. In the positive hydrophobic mismatch situation, when a hydrophobic transmembrane peptide is relatively longer than the hydrophobic thickness of a bilayer, in addition to a change in the local lipid bilayer thickness, peptide tilt, domain separation, and even repulsion of peptide from bilayer have been observed. The fact that the transmembrane peptide is shorter than the hydrophobic thickness of lipid bilayer, i.e. negative hydrophobic mismatch, suggests thermodynamic unfavorable exposure of polar residues to lipid acyl chains. Local bilayer

thickness compression near the peptide is the most likely response, although other adaptations including peptide backbone deformation, peptide oligomerization, non-lamellar phase formation, and exclusion of the peptide from bilayer have been observed.

In experimental studies of the hydrophobic matching concept, membrane systems need to be well defined and to be systematically alterable. In addition, atomic level measurement techniques need to be employed. These requirements implicate the use of simplified membrane system of well-defined composition instead of the many component biomembranes. Bloom and coworkers³³ designed hydrophobic α -helical poly-Leu peptide (L₂₄) which is capped with two hydrophilic Lys residues on each terminus to study the interaction between transmembrane peptide and lipid bilayer. In later studies³⁴, poly-Leu is replaced by a polypeptide of alternating Leu and Ala residues. Although Ala residues are less hydrophobic than Leu residues, the poly-Leu/Ala can better mimic the transmembrane protein segment than poly-Leu. Killian and coworkers³⁵ introduced poly-Leu/Ala peptides with flanked Trp-motif (WALP), which stabilizes peptide conformation by anchoring at the membrane-water interface. In investigation of peptide/membrane interactions, the designed transmembrane peptides can thus be described as a hydrophobic α -helix of poly-Leu or poly-Leu/Ala that is extended on both side with two Lys or two Trp flanked motif terminated by neutral block groups. Thickness variation on lipid bilayer in the fluid phase is achieved by the reorganization of lipid acyl chain packing. The lipid chain ordering can be experimentally determined from nuclear magnetic resonance (NMR) measurements in which the acyl chain carbons are isotopically labeled with deuterium³⁶. Lipid near the embedded protein segment extends

its length in the perpendicular direction of bilayer surface under a positive mismatch condition, resulting in increase of the order of acyl chains. Because the intrinsic time scale of the NMR measurements ($\sim 10^{-3}$ s) is longer than the typical occupancy time of a lipid near a peptide ($< 10^{-6}$ s), it is difficult to distinguish the local structure of lipids at different distances from a peptide. With spin-labeled lipids, electron-spin resonance (ESR) has been used to detect the dynamics and conformational order of lipids and verifies the conclusions drawn by NMR³⁷. A precise method of measuring the changes of lipid bilayer thickness by X-ray diffraction from oriented multilayers has been developed in a series of hydrophobic matching studies. This technique is firstly used on hydrophobic matching studies of gramicidin ion channel embedded in dimyristoylphosphatidylcholine (DMPC) bilayer or dilauroylphosphatidylcholine (DLPC) bilayer^{38,39}, then has been extended for the engineered WALP peptides at varying lengths^{40,41}. Phase separation of protein and lipids has been observed by two-photon excitation fluorescent image technique⁴². In addition, atomic force microscopy further confirmed the phase separation induced by protein in lipid bilayers⁴³.

Despite the application of advanced experimental techniques such as nuclear magnetic resonance, electron-spin resonance, X-ray crystallography, fluorescence spectroscopy, the characterization of protein-lipid systems remains difficult at atomistic level because of their intrinsic complexity. In contrast, computer simulations of membrane are capable of exploring detailed molecular structure and dynamics of system and tracking conformation changes on individual lipids, so that the order parameter on lipid acyl chains can be obtained as a function of distance to integral protein to illustrate local chain

order variations. Sperotto and Mouritsen⁴⁴ used Monte Carlo techniques with simple lattice models to simulate modeled protein-lipid system. Dramatic bilayer thickening has been found near the peptide and the thickness slowly decays in exponential form for more than 45 Å. Molecular dynamics (MD) method becomes important as speed of computer increases in studying biological membranes in the past decades⁴⁵. Woolf et al.⁴⁶ investigated hydrophobic matching mechanism by molecular dynamics simulation with WALP peptides in a lipid bilayer environment. At a 1:30 peptide:lipid molar ratio, they found that the bilayer boundary thickness increases monotonically with WALP length, as expected based on the WALP hydrophobicity. Kandasamy and Larson systematically simulated transmembrane KALP peptides (KALP15, KALP19, KALP23, KALP27, and KALP31) in DLPC, DMPC, and DPPC (dipalmitoylphosphatidylcholine) bilayers. Simulations performed at 1:25 and 1:128 peptide:lipid molar ratios revealed slower dynamics of both peptide and lipid at lower ratio. Under positive mismatch, the system alleviates the mismatch predominantly by tilting the peptide with respect to the bilayer and in a small amount by increasing lipid ordering in the immediate vicinity of the peptide. Recently, Kim and Im⁴⁷ have performed umbrella sampling molecular dynamics simulations to calculate the potential-of-mean-force (PMF) of various transmembrane α -helical peptides as a function of their tilt and rotation angles. The systematic study characterizes responses of single α -helix and lipid adaptations of hydrophobic mismatch, caused either by the hydrophobic length of peptide or by the bilayer thickness. They concluded that tilting of single helix is the major response of positive mismatch and a small inherent tilting (up to $\sim 10^\circ$ from perpendicular) remains due to helix precession even under negative mismatch.

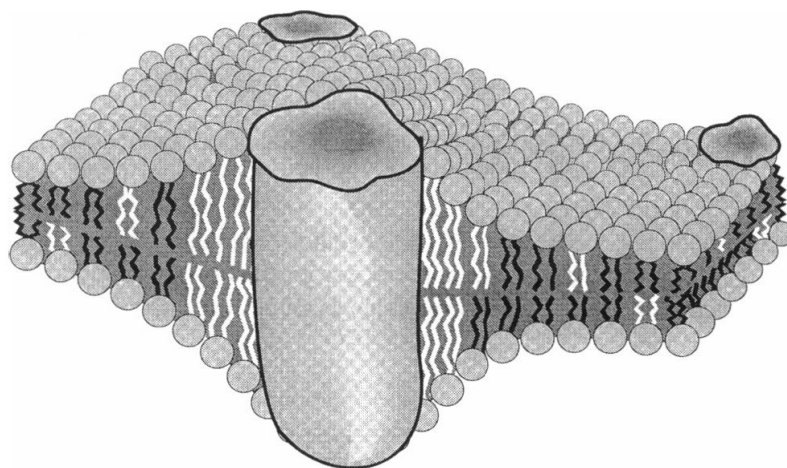


Figure 1.2. Schematic illustration of a lipid bilayer with embedded proteins and two different lipid types. Accumulation of hydrophobically best matched lipids with the transmembrane region of protein implies a lipid sorting effect at the lipid-protein interface. Adapted from ref. 48.

In membrane bilayers with two or more lipid species characterized by different acyl chain lengths, lateral redistribution of the two lipid types has been proposed as an additional perturbation to the bilayer upon protein insertion in the case of hydrophobic mismatch. A general idea is that, lipid species with the most matched hydrophobic length will be sorted around the integrated peptide in a statistical basis, and therefore have an increased probability of appearance rate in the space immediately near the peptide, as illustrated in Figure 1.2. Sperotto and Mouritsen used theoretical model and Monte Carlo method to study the distearoyl phosphatidylcholine (DSPC) and dimyristoyl phosphatidylcholine (DMPC) lipid mixture bilayer with large protein⁶. Each independent monolayer is represented by a triangular lattice array, on which each tail of a lipid occupies a site. Under the periodical boundary condition, the linear boundary between lipid and protein

crosses the simulation box, effectively making an infinite protein “wall”. Protein with $d_p = 26 \text{ \AA}$ constructed to perform simulation shows enrichment of DMPC at the protein-lipid interface. In combined theoretical and experimental studies on binary dilauroyl phosphatidylcholine (DLPC) and distearoyl phosphatidylcholine (DSPC) lipid bilayer membranes incorporating bacteriorhodopsin (BR), Mouritsen and coworkers⁴⁸ have measured the preference of BR in the mixed lipid bilayer at different physical states. Because of the large chain length difference, the two lipids have very strong nonideal demixing behavior. Standard metropolis Monte Carlo simulation technique is used to calculate the microscopic and thermodynamic properties of the theoretical model⁷ in addition to the lipid sorting around protein. With specifically designed fluorescent probes, fluorescence spectroscopy has been used to measure lipid sorting. Lehtonen and Kinnunen have observed accumulation of matched type of lipids in the immediate vicinity of integral membrane protein lactose permease from *Escherichia coli* by measuring excimer-to-monomer fluorescence intensity ratio⁴⁹. Keeffe, East, and Lee⁵⁰ have used the fluorescence quenching method to characterize the interaction between the outer membrane porin OmpF trimer from *Escherichia coli* and surrounding brominated phospholipids. The relative binding constant of OmpF for phosphatidylcholines at different acyl chain lengths shows that the lipid-protein interaction is chain length dependent, stronger binding of phosphatidylcholines with a C₁₄ chain length than those with a C₁₈. Same fluorescence quenching technique has also been used in studying interaction of potassium channel KcsA from *Streptomyces lividans* with phosphatidylcholines⁵¹. By varying the chain length in the range of C₁₀ to C₂₄, strongest relative lipid binding constants corresponding to the best hydrophobic matching are

determined. From fluorescence resonance energy transfer (FRET) measurements, Hemmingaz et al.⁵² concluded that M13 major coat protein has domain enrichment with hydrophobic matching lipid in the mixtures of the matching lipid with longer or shorter lipid. A novel photo-crosslinking method to study lipid sorting proposed by Killian et al.⁵³ can provide direct information about the packing of lipids near transmembrane peptide. In this method, a photoactivatable crosslinking probe is attached to the hydrophobic segment of a set of model transmembrane WALP peptides, and forms covalent bond between lipids upon UV irradiation light. Photo-crosslinking reaction is followed by mass spectrometry to identify lipid types binding to the peptide. Analysis result suggested lack of noticeable sorting of lipid in the presence of WALP23 α -helical peptide.

Biomembrane processes occur over a wide range of time and length scales⁵⁴, from fast process such as *trans*-gauche isomerization (10^{-10} s) of lipid acyl chains to slow process such as transformation of a single lipid from one leaflet of bilayer to the other (10^3 s). Molecular dynamics have been successfully used in studying protein and membrane interaction for the fast processes including hydrophobic matching effects. Unfortunately, the lipid sorting effect which involves lateral reorganization of lipid species over the entire system is a relatively slow process and cannot be simulated by the conventional molecular dynamics method using atomistic models without impractically long trajectories. Coarse-Grained (CG) models reduce the number of particles to represent molecules, consequently increase the simulation time scale to a level that the lipid diffusion equilibrium can be reached in MD simulations. Klein et al.⁵⁵ have engineered a

hydrophobic cylinder capped with hydrophilic sites to represent transmembrane peptide in CG model. In the mixed bilayer composed of long (DC₂₃PC) and short (DC₁₁PC) lipids, a strong preference of long lipid is observed after 1 ns MD simulation. Sansom et al. constructed CG models for engineered and known peptides including generalized alpha helical bundle and beta barrel, and embedded each peptide in two component lipid bilayers composed of long/middle or middle/short lipids⁵⁶. In the systematical MD simulation study, Sansom et al. found that the hydrophobic length preferred lipid is clearly more abundant in the first lateral shell around the peptide. Despite the efficiency of CG simulation, the lost of atomistic details in the protein-lipid interaction may not be neglected in many cases, such as a process that protein conformational changes may play an important role. Other approaches have been developed to increase simulation time scale while keeping the atomistic details of membranes. For example, hybrid- and multi-scale approaches⁵⁷ are used to overcome the simulation time limit of atomistic models. In this study, we introduce a hybrid molecular dynamics and Monte-Carlo method to accelerate lipid diffusion equilibration in mixed lipid bilayer simulations. With this method, the lateral distribution of lipids of different tail length near transmembrane protein segments can be studied at atomistic level.

1.2 Hybrid Molecular Dynamics and Monte-Carlo Methods

Despite the success of molecular simulation in study of lipids, characterization of lipid mixtures remains challenging. The lateral diffusion rate for a lipid is on the order of 10^{-12} m²/s,⁵⁸ an estimated 100 ns is needed for a lipid to migrate to a neighbor position. In a

multiple lipid component system, long-range diffusion of lipids would be needed to sample the equilibrium state, therefore, requires microsecond atomistic simulation time. The hybrid Monte Carlo (MC)/molecular dynamics (MD) method for lipid simulation method was developed by our group⁵⁹ and it has been applied to theoretical studies of membranes in different aspects⁶⁰⁻⁶³. The MC-MD method samples an isomolar semi-grand ensemble (at fixing total number of lipids, difference in chemical potential $\Delta\mu$ between the lipid components, the number of solvent and any other components, pressure, surface tension, and temperature) by attempting configurational bias⁶⁴ Monte Carlo mutation moves on a randomly selected lipid between every MD step in trajectory. The software was developed on the open-source Gromacs MD package⁶⁵ and is capable of studying the mixture of lipids that have identical headgroups but different tail length and bond types. The MC-MD method, under the regular size scale, pressure and temperature, allows a system to sample different lateral distributions of two lipids across the system much faster than through possible lateral diffusion, and equilibration may be achieved approximately two orders of magnitude faster.

1.3 Thesis Outline

In this study, the perturbation of a transmembrane peptide embedded in the binary component lipid bilayer has been systematically investigated. In chapter 2, the Neu-Erb2 transmembrane domain Neu_{TM35} was firstly introduced to test the perturbation of a peptide in a mixed lipid bilayer. Two mixed lipid bilayers composed of DSPC (di-C₁₈)-DMPC (di-C₁₄) and DMPC-DDPC (di-C₁₀) were chosen. The simulation temperature was set to 330K, which is significantly higher than the lipid gel phase melting

temperature. Observation of altering the bilayer thickness to approach the peptide hydrophobic length suggests a lipid hydrophobic matching effect. Lipid sorting effect, namely the preferred distribution of each lipid type driven by thermodynamics near the embedded peptide, is found in the mixture of DMPC-DDPC. The acyl chain length of DMPC is best matched with Neu_{TM35} peptide in the fluid phase, and is found enriched around the peptide. In order to eliminate the unraveling effect of the helical structure, harmonic positional restraint potentials were applied to all heavy atoms of the peptide. Due to the external forces of the restraint, the peptide motion such as rotation and tilt is not taken into account. This treatment then limits the simulation result to be directly compared with experimental observations, which integrates both effects contributed by both lipid sorting and peptide motion.

In chapter 3, the engineered KALP23 and WALP23 peptides were constructed to eliminate the disadvantages associated with peptide instability. KALP and WALP peptide are well studied theoretically and experimentally in different environments. In lipid bilayers, their helical secondary structures are found stable in long time scale. Moreover, the hydrophobic length of the peptide can be adjusted to match lipid bilayer thickness by increasing or decreasing the repeating unit of the peptide. Simulation results show that, without positional restraint on the peptide, both the lipid hydrophobic matching and sorting effects could not be simply explained. As the size of the peptide is of a similar scale with lipid, the peptide prefers tilting to match the hydrophobic region of the bilayer. Moreover, though the hydrophobic length of the KALP23/WALP23 is shorter

than the bilayer hydrophobic thickness, a very strong tilt still exists. This positional movement has brought difficulties to investigate both hydrophobic matching and sorting.

In chapter 4 Gramicidin A (GCA) transmembrane ion channel was incorporated in DSPC-DMPC and DMPC-DDPC mixed lipid bilayer at 1:124 peptide:lipid molar ratio. The GCA coordinates obtained from protein data bank (PDB ID: 1MAG) were determined by solid-state NMR in hydrated DMPC bilayer with 1:8 molar ratio. Our simulation study shows that GCA perturbs the bilayer thickness, in good agreement with experimental results. The β -helical GCA peptide is shorter and wider compared to the α -helices simulated in previous studies. In addition to its geometric shape, GCA has four tryptophan residues at each end of the peptide to anchor to bilayer lipid headgroups. As a result, trajectory analysis presents a weak tilting effect, but still may not be neglected. 20 ns MC-MD simulations were performed, but no significant hydrophobic sorting effects were notable. To allow relaxation of the lipid/peptide system, 20 ns conventional MD simulation starting from the previous end structure was performed, followed by another 20 ns MC-MD simulation. The improvement of sorting effect is not distinguishable between the two MC-MD segments. A factor that may obscure the sorting effect is the size and the shape of GCA.

The last chapter presents the recent hydrophobic sorting studies of outer membrane protein A of *Escherichia coli* transmembrane domain (OmpA) embedded in mixed lipid bilayers. The model peptide was constructed from the crystal structure of the OmpA transmembrane domain consisting of residues 1-171, with 2.5 Å resolution (PDB ID:

1BXW). It consists of a regular eight-stranded β -barrel, and is stable in fluid phase with water filled in the cavity. Coarse-Grained simulations were performed in a large lipid/peptide ratio (558:1 and 200:1) and strong sorting effect was observed in 2000 ns simulation time scale. Atomistic simulations adapting MCMD method reveal similar sorting effect, in a smaller system size (128 lipids and 1 peptide) and shorter simulation time scale (40 ns).

2 Atomistic Simulation of Hydrophobic Matching Effects on Lipid Distribution Near a Monomer of Neu/Erb2 Transmembrane Domain

2.1 Abstract

The hydrophobic matching effects between a transmembrane helical peptide and a two-component phospholipid bilayer were studied using a mixed molecular dynamics (MD) and configuration-bias Monte Carlo (MC) method. Atomistic simulations were applied to the Neu_{TM35} peptide embedded at a fixed perpendicular angle within a series of bilayers containing dimyristoylphosphatidylcholine (DMPC) mixed with lipids having acyl tails that are shorter by four carbons (didecanoylphosphatidylcholine, DDPC) or longer by four carbons (distearoylphosphatidylcholine, DSPC). The MCMD method works within a semigrand canonical ensemble, which allows mutation moves to transform DMPC to its counterpart and vice versa, to overcome the slow diffusion limitations of conventional MD. Strong hydrophobic matching patterns are observed in DMPC-DDPC systems over a range of mixture compositions, with both DMPC content and bilayer thickness increasing with proximity to the peptide. While inclusion of the peptide increased the mean S_{CD} order parameters of both lipid components' tails, the enrichment of DMPC in the immediate neighborhood of the peptide is reflected in a greater ordering for DMPC than for DDPC. Much weaker influence of the peptide on bilayer thickness and local composition was observed in DSPC-DMPC systems, where DSPC content is very slightly enhanced near the peptide and little difference is observed between the effects of peptide insertion on the two components' order parameters. The

degree of ordering of a lipid mixture with an embedded peptide thus appears to be a potentially useful experimental indicator of the local concentration of the lipid near the peptide.

2.2 Introduction

The interplay between the structure and energetics of lipid and protein components of biomembranes is of long-standing interest in biophysics. The “hydrophobic matching” concept has attracted significant interest in experimental, theoretical, and computational studies,²⁹ due to its simplicity and elegance as a principle to rationalize some aspects of this interplay. The basic idea is that any trans-membrane protein segment will include a section displaying a hydrophobic surface flanked by hydrophilic sections, and that the most stable peptide-bilayer interaction will occur when the length of the hydrophobic section of the peptide matches the thickness of the hydrophobic region of the bilayer. Hydrophobic mismatch, conventionally referred to as “positive” when the peptide hydrophobic length is longer than the bilayer hydrophobic thickness and “negative” for the other way around, is believed to drive conformational changes in neighboring lipids affecting the thickness of the bilayer and/or (for positive mismatch) tilting of the peptide with respect to the bilayer normal.

In a bilayer containing two or more lipid components, accommodation to a hydrophobic mismatch may further involve sorting or reorganization of the lipids, so that lipids that provide a better match to the peptide are enriched in the peptide’s vicinity. Evidence for such lipid sorting has been obtained in some experiments^{30,48}, but a recent study on a

well-characterized trans-membrane helical peptide showed sorting effects to be negligible⁵³.

Simulations, using either coarse-grained^{66,67} or atomistic^{27,46,68} representations of lipids and proteins, have provided a valuable complement to experiment in the study of hydrophobic matching effects. While the issue of lipid sorting by a transmembrane inclusion has been addressed in at least one coarse-grained model study⁵⁵, the greater computational expense of atomistic simulations makes it nearly prohibitive to perform molecular dynamics simulations long enough for lipids to reach an equilibrium distribution through lateral diffusion. For this reason, we have developed a mixed molecular dynamics-Monte Carlo approach that allows mutations between long and short-tailed lipids within the semi-grand canonical ensemble, i.e. at fixed total number of lipids and a specified difference in chemical potential $\Delta\mu$ between two lipid components⁵⁹. In a simulation box containing a peptide embedded in a lipid bilayer, the distribution of different types of lipid as a function of distance from the peptide can be monitored over the course of a simulation in which the lipids are undergoing mutation moves. As all lipids in the box are coupled to the same virtual reservoirs of the two components, the distribution of the two lipid types throughout the system converges to equilibrium with respect to the exchange of any pair of lipids. Simulation of the same lipid mixture at the same activity ratio in the absence of peptide provides a reference composition at “infinite distance”, so that even if a protein perturbs an area greater than the simulation box, a preference for one or the other kind of lipid can be discerned.

In the current study, the Neu/Erb2 transmembrane domain (Neu_{TM35}) in a two component lipid bilayer is studied. This peptide is of biomedical interest because a single mutation (Val⁶⁶⁴→Glu/Gln) greatly enhances the dimerization of the protein resulting in oncogenic activation⁶⁹. It has been the topic of a several simulation studies⁷⁰⁻⁷². A motivation of studying this peptide is to lay the groundwork toward using related methods to calculate membrane composition effects on its dimerization⁷³. The behavior of the peptide in mixtures of saturated phosphatidylcholine lipids DMPC with DDPC or DSPC are presented to show the hydrophobic matching effects between lipids with different acyl chain lengths.

2.3 Methods

2.3.1 *Molecular Dynamics and Hybrid MC-MD Setup*

Conventional molecular dynamics simulations are performed using Gromacs 3.3⁶⁵. In this study, MCMD simulations are performed according to customized Gromacs 3.3 developed by our group⁵⁹, in which use of “ghost tails” is eliminated. Protein OPLS-AA (All Atom) forcefield⁷⁴ is combined with united atom lipid forcefield of Berger et al.⁷⁵ as suggested by Tieleman et al.⁷⁶ The TIP3P model⁷⁷ of water is used for all simulations. The stochastic Langevin thermostat⁷⁸ with 2 fs integration timestep at a temperature of 330 K and a time constant of 0.1 ps was applied to MD steps. The Berendsen barostat⁷⁹ is used for semi-isotropic pressure scaling (at 1 bar pressure, zero surface tension, and time constant of 1.0 ps at assumed compressibility $4.5 \times 10^{-5} \cdot \text{bar}^{-1}$) and the particle-mesh Ewald method is used for electrostatic forces calculation during the MD step⁸⁰. Bond distances are kept constant during MD steps through the SETTLE⁸¹ and LINCS⁸² algorithms.

For each MCMD simulation, a constant ratio of thermodynamic activities of the two lipid components is used to control the composition of lipids. The activity ratio α can be represented in terms of the chemical potential difference $\Delta\mu$ as $\alpha = \exp(\Delta\mu / k_B T)$, where $\Delta\mu = \mu_{\text{DMPC}} - \mu_{\text{DDPC}}$ (or $\Delta\mu = \mu_{\text{DSPC}} - \mu_{\text{DMPC}}$). After every 2 fs MD step, a lipid is selected to perform a MC trial move of identity mutation. The acceptance probability is calculated using the configuration biased Monte Carlo algorithm⁶⁴. The average success rate is about 0.4% or 1 lipid mutation event in the system on average every 0.5 ps.

2.3.2 Configuration Construction

The atomic resolution structure of the Neu_{TM35} peptide in trifluoroethanol has been solved by NMR⁸³. The first conformation listed in the PDB file was used in this study. In neutral aqueous solution, the 35 amino-acid residues (⁶⁵⁰EQRASPVTFIATVV⁶⁶⁴GVLLFLILVVVVGILIKRRR⁶⁸⁴) are properly terminated and protonated using the *pdb2gmx* utility tool of the Gromacs, where N-terminal is NH₃⁺; C-terminal is COO⁻; glutamic acid is not protonated; one lysine and four arginines are protonated. In order to set up the initial configuration, the peptide is oriented in the center of a 6×6×6 nm cubical box, with its helical axis parallel to the *z*-axis and N-terminal pointing to the positive *z* direction.

One low energy structure of DMPC where two tails are mostly extended is used to create the lipid bilayer around the peptide. A layer of lipids containing 64 DMPCs was formed by stacking the unit cells on both *x* and *y* directions, and the place for the peptide is left

unused. The z -direction of this layer is adjusted to ensure the polar head groups of lipids contacting on the same height of the N-terminal of the peptide. Another lipid layer also containing 64 DMPC is constructed by the same procedure to cover the C-terminal, where a 180 degrees rotated DMPC unit cell is used.

Water molecules are added to the simulation box by the *genbox* Gromacs utility, and in the hydrophobic region water molecules are removed manually. 3676 water molecules are added to the system resulting in a hydration level of 28.7 water molecules per lipid.

2.3.3 Positional Constraint of Peptide in Simulation

In preliminary simulations, due to the strong interactions between the polar residues and the lipid polar headgroups, the peptide undergoes significant unraveling of the helical ends after 6 ns of simulation, up to 6 residues at N-terminus. This behavior remains even when the peptide is initially frozen and the lipids is given time to equilibrate around it. The unraveling tendency is diminished, but not eliminated, when salt (NaCl) is added to the aqueous phase to screen the coulombic interactions. Similar behavior is observed when the Gromos peptide forcefield (ffgmx) and SPC water model are used. While this unraveling is not reported in earlier published simulations of the peptide in DMPC^{70,72,84}, which also uses the experimental structure as a starting configuration, we note that the duration of those simulations are not sufficient to observe the unraveling effect. van der Ende et al.⁷¹ reported stable helices during longer simulations for both the native (10 ns) and the mutant peptide (5 ns), using the CHARMM forcefield parameters; in this case, as an electrostatic force cutoff at 11 Å is employed, the full effects of electrostatic repulsion

among the cationic N-terminus and of attraction to lipid headgroups might not have been realized.

The reason for this apparent discrepancy between simulation and experiment is not clear. It could stem from the force-field or periodic boundary conditions in the simulation. On the other hand, it could reflect real differences between the NMR structure as determined in an organic solvent environment and the structure in a bilayer; comparison of circular dichroism spectra⁸³ of the peptide suspended in bicelles and in trifluoroethanol indicates that the helical structure is maintained, but does not necessarily indicate an identical structure. In the current study, to show proof of principle of lipid sorting without interference with disordering or tilting effects, the peptide is kept at the NMR structure, with harmonic positional restraint potentials are applied to all heavy atoms of the peptide with spring constant $k = 5 \times 10^4$ kJ/mol·nm². We note that these constraints kept the peptide not only at a fixed conformation, but also at a fixed angle perpendicular to the bilayer normal.

2.3.4 *Equilibration*

The constructed 4.3×6.8×9.0 nm rectangular simulation box employs the periodic boundary condition on each direction. After energy minimization the system is equilibrated by a 10 ns MD simulation during which the anisotropic pressure coupling method is applied. The reference pressure on the *y*-direction was set higher than that on the *x*-direction, allowing *x* and *y* box dimensions to become gradually closer. Positional restraints are applied on the heavy atoms of the peptide, so that the orientation is retained

through the simulation. The conformation obtained at 9.61 ns with the smallest x - y difference where the box size becomes $6.34 \times 6.34 \times 6.45$ nm was used as a starting point for further semi-isotropic simulations. This process was repeated using DDPC lipids with a final box size of $6.49 \times 6.49 \times 5.61$ nm.

2.3.5 Simulations

MCMD simulation was performed for 20 ns (10^7 MC mutation attempts) at three activity ratios starting from the peptide-containing all-DMPC or all-DDPC structures as described above. Control MCMD runs are performed beginning with an equilibrated DMPC bilayer without peptide at the same three activity ratios. Conventional MD simulation is also performed to obtain trajectories for pure DMPC or DDPC bilayers with and without peptide.

As shown in Figure 2.1, starting from pure DMPC the composition stabilizes within 2 ns at all DMPC/DDPC activity ratio values (1.15×10^{-4} , 4.00×10^{-4} , 5.20×10^{-4}). At fixed activity ratios the overall mean compositions of DMPC/DDPC yield small but substantial differences between systems with and without peptide. Starting from 100% DMPC or 100% DDPC, Table 1 shows that DMPC has higher mole fraction in the presence of the peptide than at a center without peptide initiated with 100% DMPC. Uncertainty is calculated using the method of Wang et al⁶¹, equation 2, excluding the first 2ns equilibration period. Composition differences between runs initiated with different starting conditions exceed the calculated error bars, suggesting a residual dependence of the system composition and structure on the starting conditions. Nevertheless, the

consistently higher DMPC content of the peptide-containing systems is a first indication of an affinity of the peptide for the longer-tail lipid.

Table 2.1. Average lipid compositions at different starting configurations and activity ratios.

lipids start with	system	DMPC/lipids % in different $\alpha_{\text{DMPC/DDPC}}$		
		1.15×10^{-4}	4.00×10^{-4}	5.20×10^{-4}
all DMPC	DMPC-DDPC, peptide	25.1±0.5	55.8±0.6	63.0±0.4
all DDPC	DMPC-DDPC, peptide	23.1±0.4	53.3±0.7	61.6±0.6
all DMPC	DMPC-DDPC	22.2±0.4	51.2±0.5	60.7±0.5
		DSPC/lipids % in different $\alpha_{\text{DSPC/DMPC}}$		
		2.50×10^{-4}	1.00×10^{-3}	1.80×10^{-3}
all DMPC	DSPC-DMPC, peptide	39.2±0.7	73.7±0.4	82.7±0.5
all DMPC	DSPC-DMPC	38.5±0.4	73.5±0.6	83.4±0.4

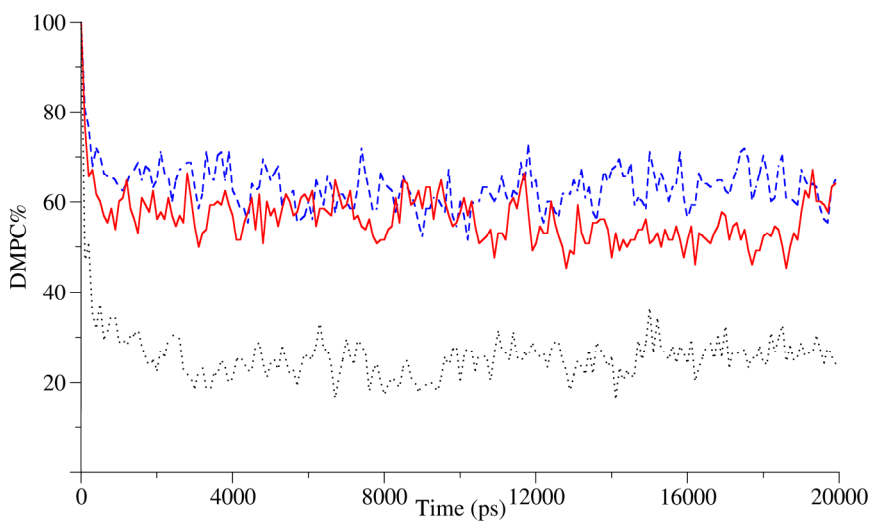


Figure 2.1. Lipid bilayer composition change against time. Blue (dash), red (solid), and black (dot) curves represent activity ratio of 5.20×10^{-4} , 4.00×10^{-4} , and 1.15×10^{-4} , for which average DMPC% are 63.0%, 55.8%, and 25.1%, respectively.

2.4 Results and Discussion

As the hydrophobic span of the Neu_{TM35} peptide placed perpendicular to the bilayer is longer than the thickness of the mixtures of DMPC and DDPC in this study, hydrophobic matching considerations lead to the prediction that the bilayer should be thicker close to the peptide than far away, and that this thickening should be promote enrichment of the longer-tail lipid DMPC in the immediate neighborhood of the peptide. The correctness of

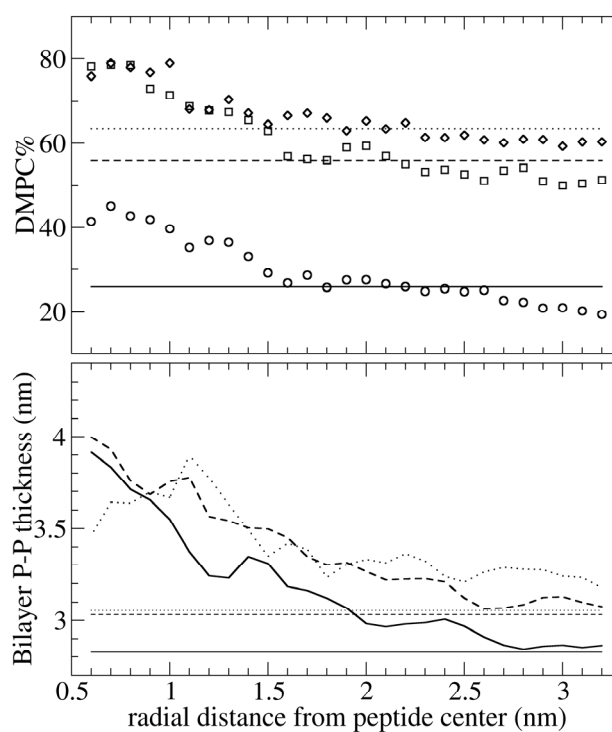


Figure 2.2. Radial distribution of DMPC-DDPC system composition (upper panel) and bilayer thickness (lower panel). Activity ratio of 5.20×10^{-4} , 4.00×10^{-4} , and 1.15×10^{-4} are dot (diamond), dash (square), and solid (circle), respectively. Control runs without peptide are shown in horizontal lines. The helical peptide is about 1.2 nm in diameter, so that lipids nearer than 0.6 nm are not counted due to poor statistics.

these predictions within the current simulations is demonstrated in Figure 2.2, which shows composition and thickness as functions of distance from the peptide center of mass in the plane of the bilayer. DMPC composition and thickness are both enhanced within a ~ 2 nm region around the peptide, consistent with the typical length scale for such peptides previously reported²⁹. The same set of simulations initialized from an equilibrated all-DDPC bilayer instead of an all-DMPC bilayer gives qualitatively similar results, confirming that this correlation of composition with position is not a kinetic artifact, e.g. of an influence of the peptide on the rate of convergence to equilibrium. Bilayer thickness is defined in terms of the difference in the average z coordinate of phosphorus atoms appearing in the upper and lower leaflets within a given lateral distance range from the peptide. Horizontal lines represent the average percent DMPC from corresponding control runs. As control runs are performed at matching activity ratios, these lines reflect the asymptotic limit of composition and thickness of bilayer regions far enough from the peptide, at equilibrium with the patch of bilayer included in the simulations including peptides. In each case, the composition and thickness at the farthest differences from the peptide within the simulation box are close to the references. This convergence to the unperturbed values suggests that the effect of periodic boundary conditions within the plane is minor. System conformations at the end of the 20 ns MCMD simulations at three different lipid compositions (Figure 2.3) are generated using VMD⁸⁵. As the distribution of lipid types is a cumulative quantity, the increased thickness and DMPC fraction near the peptide may not be significant at one instant; however, it is evident that more DMPC lipids are found around the peptide.

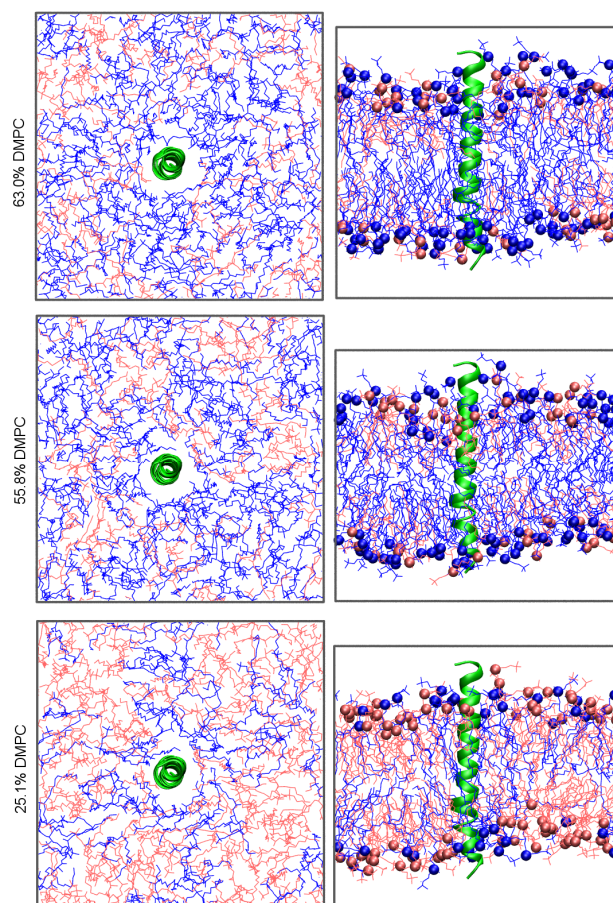


Figure 2.3. Top (left) and cross-sectional (right) views of snapshots of final simulation structures of Neu_{TM35} peptide in mixed DMPC-DDPC bilayers. Average DMPC compositions from top to bottom are 63.0%, 55.8%, and 25.1% respectively. Green, blue, and red represent peptide, DMPC, and DDPC respectively. Phosphorus atoms are shown as spheres in the right-hand panels. Water is omitted for clarity.

As the peptide is not a smooth cylinder, but rather is axially asymmetric in its distribution of side-chains, the composition may vary axially and radially in the different environments presented by different faces of the peptide. A 2-dimensional distribution of lipid composition (Figure 2.4), taking the average of all lipid sites with 0.1 nm resolution, shows that the enhancement of long-chain lipids is direction specific, particularly at low DMPC concentration. Comparison with the control images suggests that these variations

are more pronounced than thermal fluctuations in the absence of the peptide. The specifics of this axial distribution are not consistent, however, between the runs initiated with different starting compositions (data not shown). This inconsistency suggests that the observed behavior of the first shell of lipids interacting with the peptide is governed to some extent by initial conditions and is not well equilibrated over 20 ns simulation.

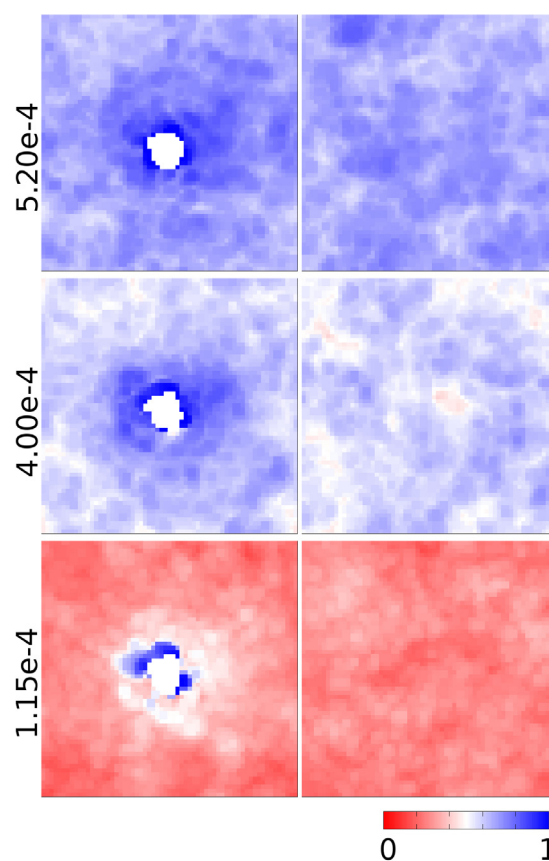


Figure 2.4. Lateral atomistic distribution of DMPC over lipids. Left column is for systems with peptide; right column is for system without peptide. Presented activity ratios from bottom to top are 1.15×10^{-4} , 4.00×10^{-4} , and 5.20×10^{-4} , respectively.

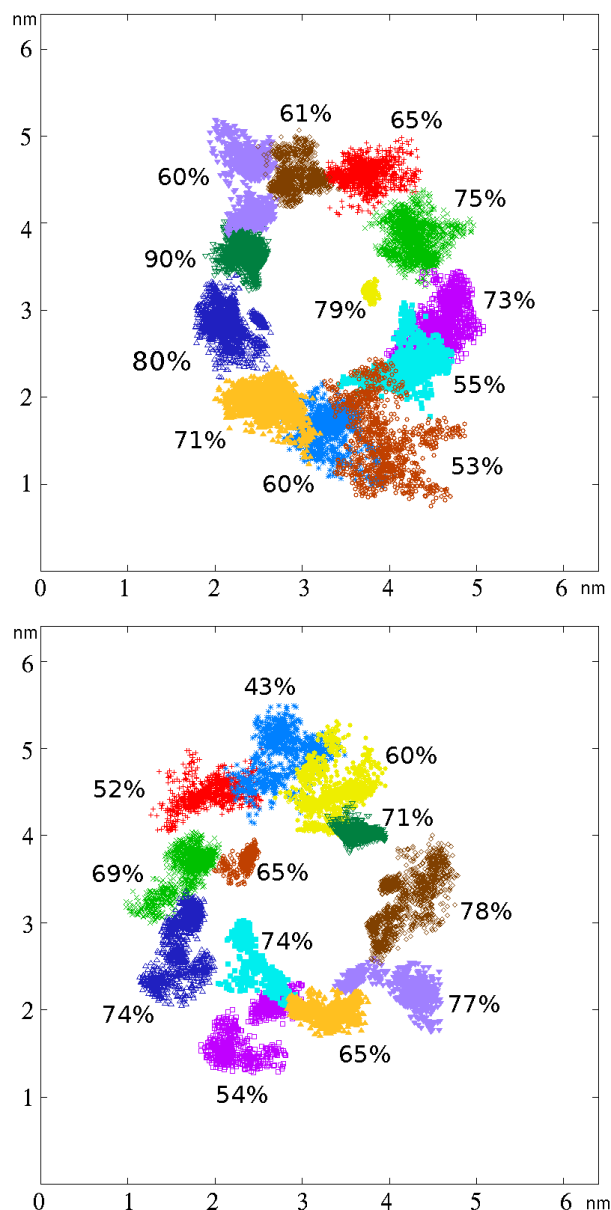


Figure 2.5. Scatter plot of lipid phosphorus atom positions for lipids near the peptide in upper (upper panel) and lower (lower panel) mono layer for simulation with 55.8% DMPC, 44.2% DDPC. The fraction of time spent as DMPC is marked for each lipid beside its colored patch.

Scatter plots of the lateral positions of phosphorus atoms provide further insight into the behavior of individual lipids near the peptide. The plots for the 12 lipids nearest to the peptide in each leaflet for an activity ratio of 4.0×10^{-4} are shown in Figure 2.5. The

appearance of phosphorus atoms generates a nearly rounded empty area occupied by the peptide. The diffusion of a lipid is not significant in 20 ns time scale, and most of them stay in areas between 0.5 to 2 nm across. Patches smaller than the average size appear near the center on both layers. The tight distributions of phosphorus atom positions suggest that lipid headgroups are very strongly associated with the peptide. Investigation of simulation snapshots shows that the polar head groups of these lipids bind to charged sites on the hydrophilic end of the peptide and do not move away during the simulation time. The use of tail mutation moves does not directly aid in accelerating the equilibration of the headgroup arrangements. If headgroup configurations are slow to relax as in the present case and sensitive to the composition, a true equilibrium may not be reached even after multiple tail-group mutations.

Results on DMPC-DSPC mixtures are summarized in Figure 2.6. Of the three DMPC-DSPC mixtures modeled, the one with the highest percentage of the longer-tail DSPC component shows no evidence of hydrophobic matching effects in either thickness or composition dependence on distance from the peptide. From this we conclude that the 80:20 DSPC-DMPC mixture, with thickness of approximately 4.2 nm as measured between the phosphorus sites, is close to optimal for this peptide. For the run with the lowest DSPC content, weak trends qualitatively similar to the DMPC-DDPC mixtures could be discerned; the bilayer thickness enhancement is under 0.5 nm, and the enrichment of the long-chain component is at most 10%. At the intermediate composition, results are ambiguous. These results are consistent with a non-linearity in the free energy penalty for hydrophobic mismatch: because lipid sorting is more

pronounced for C_{10}/C_{14} tail lipid mixtures than for C_{14}/C_{18} tail lipid mixtures, we can infer that the penalty for substituting a C_{10} tail lipid with a C_{14} tail lipid next to the peptide is greater than for substituting a C_{14} tail lipid with a C_{18} tail lipid.

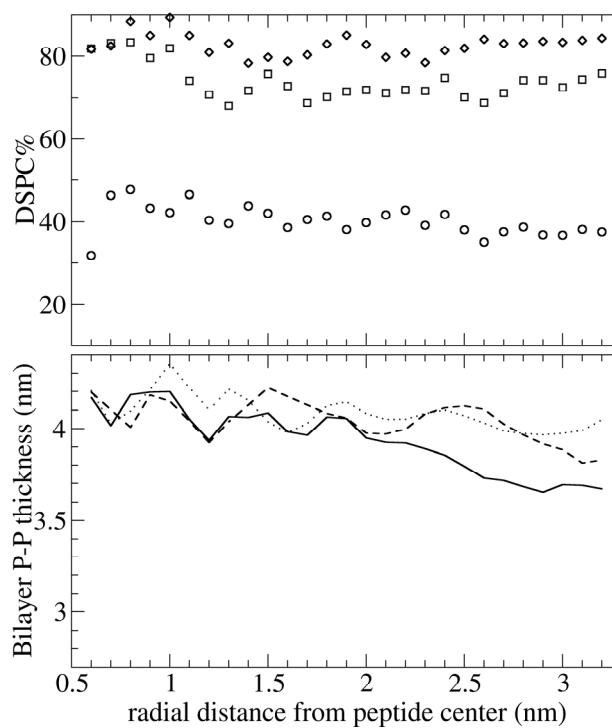


Figure 2.6. Radial distribution of DMPC-DSPC system composition (upper panel) and bilayer thickness (lower panel). Activity ratio of 2.5×10^{-4} , 1.00×10^{-4} , and 1.8×10^{-4} are solid (cycle), dash (square), and dot (diamond), respectively.

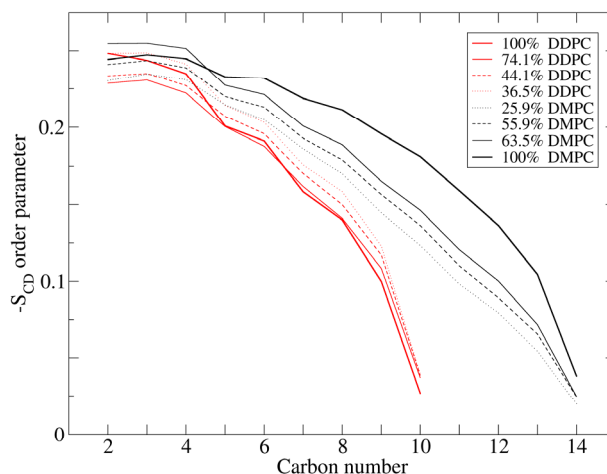


Figure 2.7. C-H bond order parameters for methylene and methyl groups of lipid acyl tails by position in the tail, averaged over all protons on both tails.

Carbon-hydrogen (or carbon-deuterium) bond order parameters, commonly denoted S_{CD} , are commonly determined via NMR as a measure of lipid bilayer structure. Here we attempt to use our simulation results to determine whether order parameters reflect lipid sorting. Order parameters for methylene groups in lipid acyl chains for the lipid/peptide mixtures at various DMPC/DDPC ratios are shown in Figure 2.7. As observed in an experiment⁸⁶ and in previous MCMD simulations⁵⁹, the degree of order of both components in mixed-tail length bilayers increases as the fraction of long-tail component increases. Here we focus on the response of the two components to the presence of the peptide, as a convenient experimental probe of the lipid response. Due to the use of a simulation method in which the composition is determined through an equilibrium process of mutation moves, it is difficult to compare systems with identical lipid composition in the presence and absence of peptide, which would be the natural comparison in an experiment. However, as the composition differences between

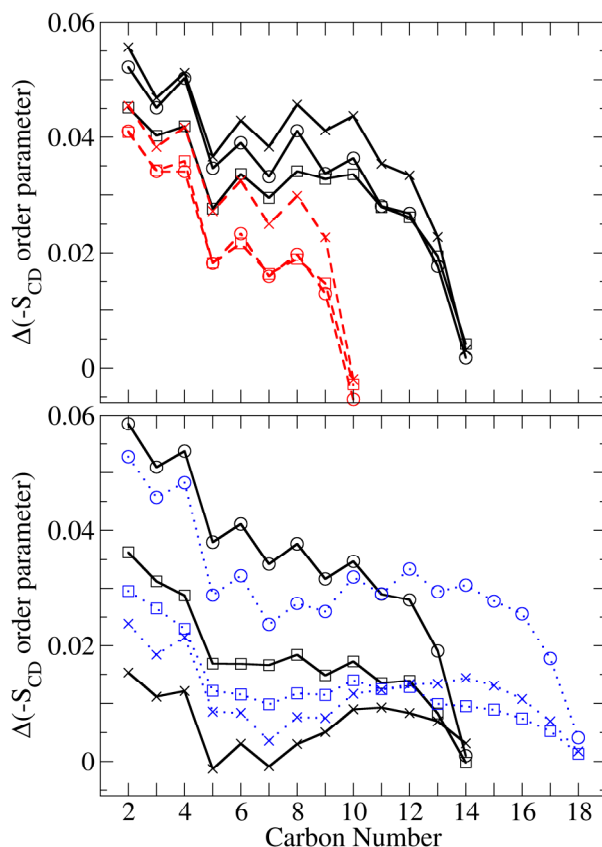


Figure 2.8. C-H bond order parameter differences between system with peptide and without peptide. Red (dash) lines represent DDPC; black (solid) lines represent DMPC; blue (dot) lines represent DSPC. On the upper panel (DMPC-DDPC mixture), circle, square, cross represent data for 25.1%, 55.8%, and 63.0% DMPC, respectively. On the lower panel (DMPC-DSPC mixture), circle, square, cross represent data for 39.2%, 73.5%, and 83.4% DSPC, respectively.

runs with and without peptide do not exceed 3-5% (see Table 2.1), the effect of composition alone is much less important than the contribution to ordering from the peptide; we therefore determined the difference in order parameters for each component of lipid mixtures with and without peptide at fixed activity ratio (Figure 2.8). In general, the enhancement of order induced by the peptide is greater for carbons near the headgroup. In DMPC-DDPC mixtures (upper panel), it is apparent that the addition of

peptide increases the order parameters of DMPC lipid tail methylene groups by about 0.01 units more than the increase to DDPC order parameters. In DSPC-DMPC mixtures, the addition of peptide has a smaller total effect on order parameters, and the effect is approximately the same for the two components. The thickening of the bilayer requires greater extension of lipid tails, and accordingly increases order of lipids. The difference between the lipid components' responses is much greater in the DMPC-DDPC mixtures, where the DMPC is strongly enriched near the peptide, than in the DSPC-DMPC mixtures, where the lipids are nearly evenly distributed. We propose, therefore, that such differences in lipid components' ordering response to the presence of peptide can provide useful evidence for experimental measurements of lipid sorting.

The results of the MCMD simulations are all consistent with the idea that a positive hydrophobic mismatch induces an enrichment of longer-tail lipids near a transmembrane helix. However, they are in apparent contradiction to a direct experimental test of hydrophobic matching-driven sorting effects, in which a photolabile group is attached to a transmembrane helical peptide to covalently capture lipids in contact with the peptide⁵³. Photo-crosslinking study evidently shows that, in a homogeneously mixed fluid phase of DSPC (C_{18}) and DLPC (C_{12}) lipids at 333 K, the photolabile WALP peptide is crosslinked to long and short lipids in direct proportion to their mixing fractions, therefore hydrophobic matching considerations could predict an enhancement of the DSPC. One likely source for this discrepancy is the use of constraints on the peptide in the present simulations to prevent the peptide from accommodating to the bilayer thickness through tilting, which would reduce the driving force for lipid sorting. Indeed,

a simulation-assisted reinterpretation of experimental data on the WALP + DMPC system suggests that the peptide used in the cross-linking experiments may be tilted to a greater degree than anticipated⁸⁷. While the neglect of tilting and other degrees of freedom makes it difficult to compare the current simulation results with experimental data on transmembrane peptides, the constraint of a transmembrane peptide segment to a fixed orientation is not necessarily unphysical: when attached to a bulky solution domain, for instance, a transmembrane helix may be restricted to tilt. With the choices of peptide and lipids in the current simulations, we are unable to access the “negative” hydrophobic matching regime, where a local thinning of the bilayer is predicted and tilting does not play a role.

2.5 Conclusions

Molecular dynamics simulations and mixed molecular dynamics / Monte Carlo simulations of the Neu_{TM35} peptide in DMPC, DDPC, DSPC, and their mixtures thereof are performed. In preliminary conventional MD simulations initiated with a reported NMR structure, the peptide in pure DMPC bilayer shows unraveling of highly charged hydrophilic ends of the peptide, suggesting that peptide in organic solvent may be more ordered than does lipid bilayer-associated peptide. In further simulations, the transmembrane peptide is constrained to its experimentally determined structure and held perpendicular to the membrane to give the most favorable circumstances for lipid sorting. Under these conditions, the peptide induces a non-random distribution of lipids in which the longer-tail lipids are enriched near the peptide in accordance with the principles of hydrophobic matching. The enrichment is greater in DMPC-DDPC mixtures than in

DSPC-DMPC mixtures. As the most directly perturbed component in the DMPC-DDPC mixtures, the DMPC experiences a greater-increase in tail methylene order parameter than does the shorter-tail DDPC upon addition of the peptide; in DSPC-DMPC mixtures where sorting is much less evident, the peptide induces similar changes in order parameter to the two components. The constraints on the peptide in this case are somewhat artificial, as accommodation of positive hydrophobic mismatch through tilting would be expected to remove the driving force for lipid sorting, but the prediction of significant sorting would apply to cases involving a larger protein or protein assembly where the orientation of the transmembrane section is subject to geometric or steric constraints.

The MCMD method facilitates the attainment of a non-randomly mixed lipid bilayer with much shorter trajectories and less computational expense than the microsecond-long MD trajectories that would be required for demixing via lateral diffusion alone. The simulation results highlight that the use of mutation moves accelerates one dynamic degree of freedom in the system – the exchange of a lipid of one type with a lipid of the other type – leaving other slow processes to become rate-limiting. In the present case, the exchange of lipid headgroup associations with hydrophilic sites on the peptide, which is necessary to relax the axial distribution of lipids around the helix, is slow on the 20 ns simulation timescale. Nonetheless, the method has potential to yield qualitative predictions and microscopic insights into protein-induced lipid sorting in a wide variety of systems.

3 Hydrophobic Sorting Effect Studies with Engineered WALP/KALP Alpha Helices

3.1 Introduction

Hydrophobic sorting has attracted attention in biological membrane studies for many years. Due to complexity of real membrane environments, simplified models are widely used to address the lipid domain aggregation under different physical conditions. In these models, a transmembrane peptide is embedded in a lipid bilayer consisting of two types of lipid that are different in their acyl tail lengths. Early theoretical studies⁶ investigated the DSPC-DMPC mixture perturbed by an imaginary infinite wide transmembrane peptide. Theoretical calculation on the free energy changes forecasts the preference of DMPC near the peptide, and Monte Carlo simulation confirms the prediction. Though this model system is elegant and the lipid sorting is consentient, the assumption of the infinite size of peptide is too arbitrary to be used for a realistic system. Hydrophobic matching mechanism has been investigated by molecular dynamics with WALP peptides (16, 17, 19, 21, and 23 residues) in pure DMPC or DPPC bilayers⁴⁶. Authors have found that the peptide-lipid packing and peptide tilt depend not only on peptide length but also on the relative positions of Trp residues around the helix axis on each terminus. Direct experimental measurement of sorting by photo-crosslinking⁵³ of WALP peptide and DSPC-DLPC lipid bilayer mixture suggests that no preference of any moiety is notable in the direct contact with the WALP peptide on some selected residue for the covalent bonding. In this chapter we use hybrid molecular dynamics and Monte Carlo methods to

investigate the systems of mixed DSPC-DMPC and DMPC-DDPC with WALP23 and KALP23 peptide in full hydrated environment.

3.2 Method

The WALP peptide family that has been extensively used in experimental studies of the hydrophobic matching mechanism is constructed as an alternating sequence of Leu and Ala residues of various lengths, terminated by a pair of Trp residues at each end. The WALP23 peptide is formyl-Ala-Trp-Trp-(Leu-Ala)₈-Leu-Trp-Trp-Ala-ethanolamine. KALP23 peptide has the same sequence except replacement of Trp with Lys at each end. The structure of WALP23 and KALP23 are constructed with an ideal alpha helical peptide backbone followed by mutation of side chains to corresponding residues. The capping of C-terminal of peptide with ethanolamine and amide derives different behaviors in practice⁸⁸, so both capping methods are used in simulations. All the simulated temperatures of system in the present study are listed in Table 3.1. Forcefield parameter is generated by Gromacs *pdb2gmx* tool with OPLS option. The peptide is added into equilibrated bilayers containing 128 lipids in the present study followed by removal of overlap lipids and waters molecules, and the system is the energy minimized. Conventional MD simulations are performed for each system, and MCMD simulations are performed for all mixed lipid systems.

Table 3.1. Simulated temperatures of systems mixed with peptide and lipids.

	WALP-NCCOH	WALP-NH2	KALP-NCCOH	WALP-NH2
DSPC	330K	300K, 330K	330K	330K
DSPC-DMPC	330K	300K, 330K	330K	330K
DMPC	330K	300K, 330K	330K	330K
DMPC-DDPC	330K	300K, 330K	330K	330K
DDPC	330K	300K, 330K	330K	330K

3.3 Results and Discussion

The mobility of the WALP/KALP peptide is significant. In all simulated systems, peptide exhibits strong tilt to compromise the lipid bilayer deformation for hydrophobic matching. Figure 3.1 shows the snapshot of WALP23-NH2 in pure DDPC bilayer. The Trp residue which acts as an anchoring point to interact with lipid headgroups on the bilayer surface does not provide sufficient force for the peptide to remain its orientation. As the motion on the peptide is higher than the rate of lipid diffusion, the sorting of lipid is not noticeable in mixed lipid bilayers. Figure 3.2 shows the radial distribution of DMPC in the DMPC-DDPC/WALP23-NH2 system. In theory, the ratio of a better matched lipid, DDPC in this case, is more energetically favored. The distribution function shows a strong fluctuation near the peptide and the ratio of DDPC is more abundant in the far away range.

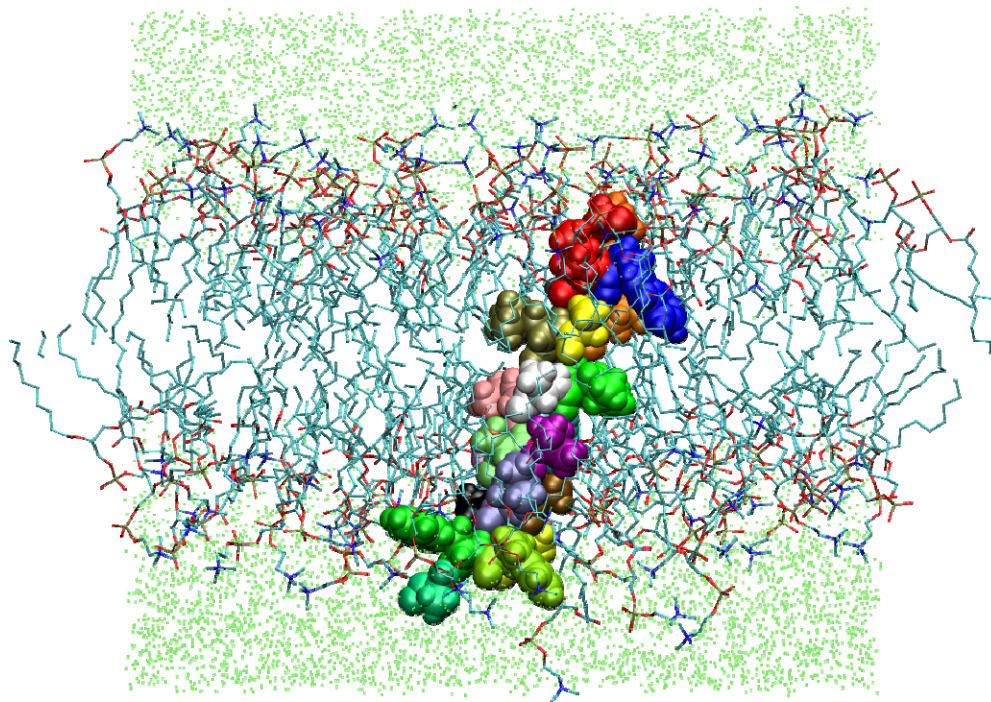


Figure 3.1. Snapshot at 20 ns for WALP23-NH2 peptide in DDPC bilayer at 330K.

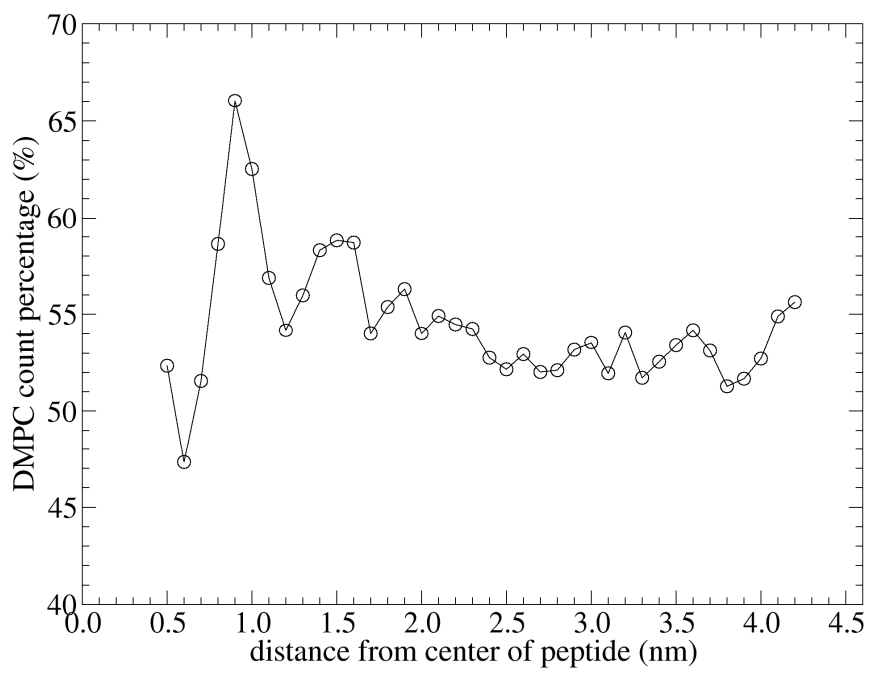


Figure 3.2. Radial distribution of DMPC in the DMPC-DDPC/WALP23-NH2 system.

3.4 Conclusions

The WALP23 and KALP23 peptide are simulated in pure and mixed lipid bilayers. Rapid peptide tilt is observed in all simulated systems, in which lipid bilayer thickening or thinning is not the dominant factor to accommodate hydrophobic matching. Hydrophobic sorting as a derivative from hydrophobic matching to adapt the perturbation of transmembrane peptides would not be a primary factor of interactions between protein and lipids. Future studies of hydrophobic sorting may require a peptide having a stable orientation in lipid bilayer, that the sorting of lipids is a dominant contributor to system assembly.

4 Atomistic Simulation of Hydrophobic Sorting Effects Near Beta Helix: the Gramicidin A Transmembrane Ion Channel

4.1 Abstract

The local lipid composition near a transmembrane helical peptide in mixed-lipid bilayers has been studied using a mixed molecular dynamics (MD) and configuration-bias Monte Carlo (MC) method that allows the lateral distribution of lipids to equilibrate much more quickly than is possible by diffusive mixing alone. Gramicidin-A peptide was embedded in bilayer mixtures of DMPC with either DDPC (shorter by four carbons per tail) or DSPC (longer by four carbons per tail) at 330 K to investigate the possibility of lipid sorting by tail length. Conventional MD simulations showed local thickening of the bilayer near the peptide in pure DDPC and local thinning of the bilayer in pure DSPC, with comparatively little perturbation to the thickness of pure DMPC bilayers, suggesting that DMPC has the best matched tail length to the peptide of these three. In 1:1 DMPC:DDPC mixtures, the DMPC lipid was weakly enriched (by about 5%) near the peptide, while in DMPC:DSPC mixtures no consistent trend was observed. The results underscore the weakness of the coupling between membrane deformation and local composition fluctuations in the absence of spontaneous phase separation.

4.2 Introduction

The interplay between the structure and energetics of lipid and protein components of biomembranes is of long-standing interest in biophysics. The “hydrophobic matching”

concept has attracted significant interest in experimental, theoretical, and computational studies,^{29,89} due to its simplicity and elegance as a principle to rationalize some aspects of this interplay. The basic idea is that any trans-membrane protein segment will include a section displaying a hydrophobic surface flanked by hydrophilic sections, and that the most stable peptide-bilayer interaction will occur when the length of the hydrophobic section of the peptide matches the thickness of the hydrophobic region of the bilayer. Hydrophobic mismatch, conventionally referred to as “positive” when the peptide hydrophobic length is longer than the bilayer hydrophobic thickness and “negative” for the other way around, is believed to drive conformational changes in neighboring lipids affecting the thickness of the bilayer and/or (for positive mismatch) tilting of the peptide with respect to the bilayer normal. Thickness fluctuations are inevitably associated with curvature effects, and these correlations can lead to non-monotonic relaxation of thickness vs. distance from the perturbing peptide⁶⁶ and long-range attractions between peptides⁹⁰.

In a bilayer containing two or more lipid components, accommodation to a hydrophobic mismatch may further involve sorting or reorganization of the lipids, so that lipids that provide a better match to the peptide are enriched in the peptide’s vicinity³⁰.

Experimental evidence for such lipid sorting has been obtained in some experiments, but only in systems where the lipids themselves undergo phase separation. Dumas et al.⁴⁸ reported the lipid sorting effect in the mixture of DLPC and DSPC by bacteriorhodopsin (BR) through fluorescence energy transfer to a lipid-soluble probe. At 263 K or 293 K, BR is clearly associated with DLPC-rich domains in gel-gel and gel-fluid coexistence

regimes, while in the fluid-phase mixture at 338K any difference in association was too weak to measure (but was predicted using lattice MC simulations). Fahsel et al.⁹¹ studied the lateral membrane organization and phase behavior of DMPC and DSPC of a mixture of gramicidins using neutron scattering, infrared spectroscopy and fluorescence microscopy, and found a preference for the DMPC-rich phase in the mixture under both gel-fluid and gel-gel coexistence conditions. A photo-crosslinking study on the WALP23 helical peptide within several mixtures of longer and shorter tailed lipids (including DLPC-DSPC) showed sorting effects to be significant in the two-phase region but undetectable in homogeneous fluid-phase mixtures⁵³.

Simulations, using either coarse-grained^{66,67} or atomistic^{27,46,68} representations of lipids and proteins, have provided a valuable complement to experiment in the study of hydrophobic matching effects. While the issue of lipid sorting by a transmembrane inclusion has been addressed in at least one coarse-grained model study⁵⁵, the greater computational expense of atomistic simulations makes it nearly prohibitive to perform molecular dynamics simulations long enough for a mixture of lipids to reach an equilibrium distribution through lateral diffusion. For this reason, here we use a mixed molecular dynamics-Monte Carlo approach that allows mutations between long and short-tailed lipids within the semi-grand canonical ensemble, i.e. at fixed total number of lipids and a specified difference in chemical potential $\Delta\mu$ between two lipid components⁵⁹. In a simulation box containing a peptide embedded in a lipid bilayer, the distribution of different types of lipid as a function of distance from the peptide can be monitored over the course of a simulation in which the lipids are undergoing mutation

moves. As all lipids in the box are coupled to the same virtual reservoirs of the two components, the distribution of the two lipid types throughout the system converges to an equilibrium lateral distribution with respect to the exchange of any pair of lipids.

Simulation of the same lipid mixture at the same activity ratio in the absence of peptide provides a reference composition at “infinite distance”, so that even if a protein perturbs the local composition over an area greater than the simulation box, a preference for one or the other kind of lipid can be detected.

In the current study, gramicidin A (GCA) transmembrane ion channel is simulated in two-component mixed-lipid bilayer. GCA is modeled in a head-to-head polypeptide dimeric form that consists of two identical chains, each containing 17 residues (Fm-VGALAVVVWLWLWLW-Etn), where the alternation of D- and L-valine and leucine promotes the formation of β helix. Its tendency to perturb the thickness of host bilayers, presumed due to hydrophobic matching effects, has been studied experimentally. Using NMR methods at a 1:30 peptide:lipid ratio and at 10 K above the main phase transition temperature of each lipid, de Planque et al. measured increases in bilayer thickness upon GCA insertion for DLPC, DMPC, and DPPC, respectively (suggesting positive hydrophobic mismatch) and a small decrease for DSPC (suggesting negative mismatch)³⁷. Huang et al. also measured the thicknesses of gramicidin embedded in fluid-phase DMPC or DLPC bilayers at a 1:10 peptide/lipid ratio by x-ray diffraction³⁸, and observed that the presence of gramicidin increased the thickness of DLPC and decreased the thickness of DMPC. In the present work, the fluid-phase mixtures of DMPC-DDPC or DMPC-DSPC with GCA are studied, with the intention of capturing

both positive and negative mismatch regimes. Lipid demixing in the presence of peptide according to the hydrophobic matching effects between lipids with different acyl chain lengths is discussed.

4.3 Methods

4.3.1 *Simulation*

Conventional molecular dynamics simulations are performed using Gromacs 3.3⁶⁵.

MCMD simulations are performed according to the method in our group recent publication⁵⁹ using GIMLi, a customized version of Gromacs 3.3

(http://www.chemistry.emory.edu/faculty/kindt/GIMLi_v1.htm). The combination of protein OPLS-AA (All Atom) forcefield⁷⁴ with united atom lipid forcefield of Berger et al.⁷⁵ was used as suggested by Tieleman et al.⁷⁶ The TIP3P model⁷⁷ of water is used for all simulations. The stochastic Langevin thermostat⁷⁸ with 2 fs integration timestep at a temperature of 330 K and a time constant of 0.1 ps was applied on MD steps. The Berendsen barostat⁷⁹ was used for semi-isotropic pressure scaling (at 1 bar pressure, zero surface tension, and time constant of 1.0 ps at assumed compressibility $4.5 \times 10^{-5} \text{ bar}^{-1}$) and the particle-mesh Ewald method for electrostatic forces calculated during the MD step⁸⁰. Bond distances are kept constant during MD steps through the SETTLE⁸¹ and LINCS⁸² algorithms.

MCMD simulation is performed as in reference 16, using the GIMLi. A constant ratio of thermodynamic activities (i.e., fugacities) of the two lipid components is used to control the composition of lipids. The activity ratio α can be represented in terms of the chemical

potential difference as $\alpha = \exp(\Delta\mu/k_B T)$, where $\Delta\mu = \mu_{\text{DMPC}} - \mu_{\text{DDPC}}$ (or $\mu_{\text{DMPC}} - \mu_{\text{DDPC}}$). After every 2 fs MD step a lipid is selected to perform a MC trial move of identity mutation. The new configuration and the acceptance probability are calculated using the configuration biased Monte Carlo algorithm⁶⁴. The average success rate is about 0.4% or 1 lipid mutation event in the system on average every 0.5 ps.

A high resolution structure of the CGA peptide in DMPC bilayer has been obtained with solid-state NMR⁹² and was downloaded from Protein Data Bank (1MAG) as the starting structure. Forcefield configuration of formyl and ethanolamine groups are modified to allow them to link with peptide termini, and Gromacs *pdb2gmx* utility tool was used to build the topology file where N-terminus is capped with formyl and C-terminus is capped with ethanolamine.

4.3.2 System Construction

An initial structure of peptide embedded system is constructed with an algorithm developed by Tieleman et al.⁹³. A DMPC bilayer patch that composed of 128 lipids and 3655 waters which has been completely equilibrated in the fluid phase was used to build the starting configuration of lipid peptide system. The bilayer is in a 6.4×6.4×6.2 nm box, where the lipid bilayer norm points to the *z* direction. To place the GCA peptide into the bilayer, GCA is first rotated to the direction where its principal axis is parallel to *z* axis. The peptide is also translated to the center of the box on *x-y* plane, and on the *z*-direction the peptide is placed on the middle of lipid bilayer. Secondly, the overlapped lipids are removed through an expansion and removal procedure. In the expansion procedure, all

molecules are translated to new positions where their center of mass coordinates on x and y are 10 times of their original value. Four lipids nearest to the peptide, two on each bilayer leaflet, are removed to eliminate lipid-peptide overlap at the current expanded sparse state. Then expanded configuration is compressed to restore to its original position by 14 sequential steps with a multiplication factor of 0.95 on x and y at each step. Energy minimization of the entire system is applied after each translational step, so that lipids that may still overlap with the peptide can adjust their positions. Finally, the original number of waters is added back into the system, giving a hydration level of 29.5 waters per lipid. This process is repeated to build systems containing all DSPC or DDPC lipids instead of DMPC.

Each constructed initial system is equilibrated by a 2 ns MD simulation during which the motion of peptide atoms is restrained by harmonic potentials. Started with the equilibrated structure, a 20 ns conventional MD production run is performed and the peptide restraint is removed. Subsequently, MCMD studies are performed to obtain mixed-lipid systems (DSPC-DMPC and DMPC-DDPC), where the lipid components only differ by 4 alkyl carbons on their tails. From preliminary MCMD simulations, the activity corresponding to a 1:1 proportion of lipid types were estimated to be 4.00×10^{-4} for DSPC-DMPC and 3.87×10^{-4} for DMPC-DDPC. For both mixtures, two independent trajectories were run, one starting from 100% long-tail lipids and the other starting from 100% short-tail lipids. After 20 ns of MCMD, the convergence of lipid composition appeared to be slower in the presence of the peptide than seen previously without peptide, the peptide dynamics apparently limiting the rate of convergence. To promote relaxation

of the peptide/lipid system, a 20 ns interval of pure MD was then carried out for each system. (Conventional MD rather than MCMD was used for this interval to allow simulation in parallel, which is not yet a working option for the GIMLi MCMD code.) A second round of 20 ns of MCMD simulation was then performed and used for data analysis. Conventional MD simulations are also performed to obtain controls of pure lipid bilayers with and without peptide.

4.4 Results and Discussion

4.4.1 *Hydrophobic matching*

Starting from 100% each type of lipid, Table 1 shows the average composition of the systems in the present work. Uncertainty is estimated using the method of Wang et al.⁶¹ (equation 2) with the second MCMD simulation trajectories. DSPC-DMPC/GCA system compositions are converged for systems starting from all DSPC or all DMPC lipids initial configurations, which approximately equal to the value obtained from control run. Peptide-containing DMPC-DDPC mixtures system started from all DMPC showed moderately 2% DMPC content than either the peptide-free control or the peptide-containing system started from all DDPC.

Table 4.1. Average lipid compositions at different starting configurations and activity ratios in binary lipid mixtures.

mutation start with	system	%long tail lipids / all lipids	activity ratio
all DMPC	DSPC-DMPC	50.0 ± 0.4	4.00×10^{-4}
all DSPC	DSPC-DMPC, GCA	50.8 ± 0.6	4.00×10^{-4}
all DMPC	DSPC-DMPC, GCA	49.8 ± 0.7	4.00×10^{-4}
all DMPC	DMPC-DDPC	51.2 ± 0.5	3.87×10^{-4}
all DMPC	DMPC-DDPC, GCA	53.0 ± 0.4	3.87×10^{-4}
all DDPC	DMPC-DDPC, GCA	51.0 ± 0.4	3.87×10^{-4}

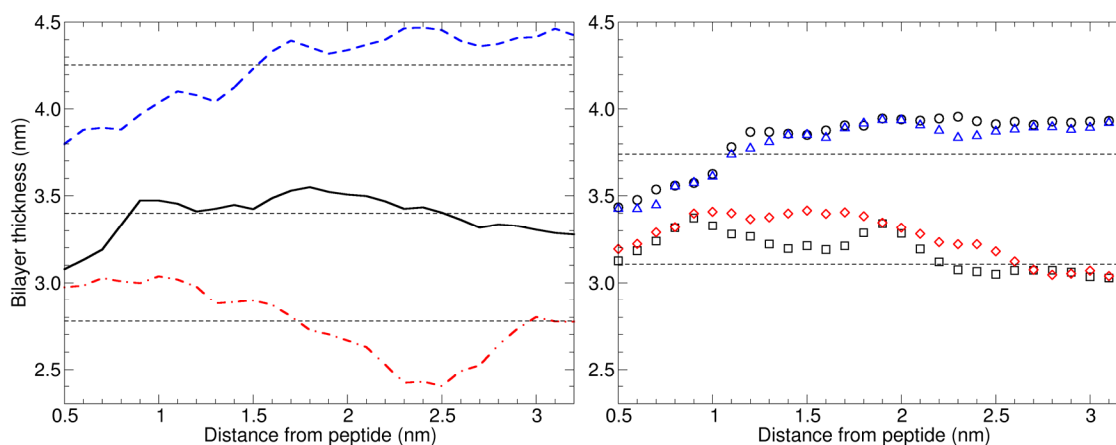


Figure 4.1. Lipid bilayer thickness as radial distance to the center of mass of peptide. Left panel shows the pure lipid bilayer with GCA, in which blue dash, black solid, red dash-dot lines represent systems with DSPC, DMPC, DDPC, respectively. Horizontal dash lines represent the average thickness for the control systems, starting from top: DSPC (4.26nm), DMPC (3.40nm), DDPC (2.78nm), respectively. Right panel shows the mixed lipid bilayer with GCA. Black circle and blue triangle represent the mixed DSPC-DMPC system, starting with all DSPC or DMPC, respectively. Black square and red diamond represent the mixed DMPC-DDPC system, starting with all DMPC or DDPC, respectively. Horizontal dash lines represent the average thickness for the control systems, starting from top: DSPC-DMPC (3.74nm), DMPC-DDPC (3.11nm), respectively.

As the hydrophobic span of the GCA peptide placed perpendicular to the bilayer is longer than the thickness of DMPC and DDPC³⁸, and shorter than the thickness of DSPC in this study, hydrophobic matching considerations lead to the prediction that the bilayer should be thicker close to the peptide than far away in DMPC and DDPC, and vice versa. We use the center-of-mass distance of the lipid head groups on each leaflet along the bilayer normal to calculate the bilayer thickness. Figure 4.1 displays the thickness of all simulated systems as a function of lateral distance r from the center of peptide, starting from 0.5 nm (radius of the peptide cross area) to 3.2 nm (box edge). Pure DSPC, DMPC and DDPC are 4.26, 3.40, 2.78 nm thick respectively without the presence of GCA. The presence of the embedded GCA significantly influences the thickness of lipid bilayer. In the DSPC/GCA system, the bilayer thickness sharply increases from 3.80 nm at $r = 0.5$ nm to 4.39 nm at $r = 1.7$ nm and reaches 4.42 at $r = 3.2$ nm, indicating strong thinning of DSPC near the peptide, indicating negative hydrophobic mismatch. In contrast, in the DDPC/GCA system positive hydrophobic mismatch is observed: bilayer thickness slightly fluctuates between 2.97 and 3.03 nm (0.22 nm greater than control) for $r < 1.2$ nm, and sharply decreases to 2.40 nm (0.38 nm less than control) at $r = 2.5$ nm. The medium length DMPC has less strong hydrophobic matching effect comparing with DSPC and DDPC. The thickness of DMPC/GCA increases from 3.08 at $r = 0.5$ nm to 3.47 at $r = 0.9$ nm, which is slightly greater than control, and levels off at $r = 2.5$ nm.

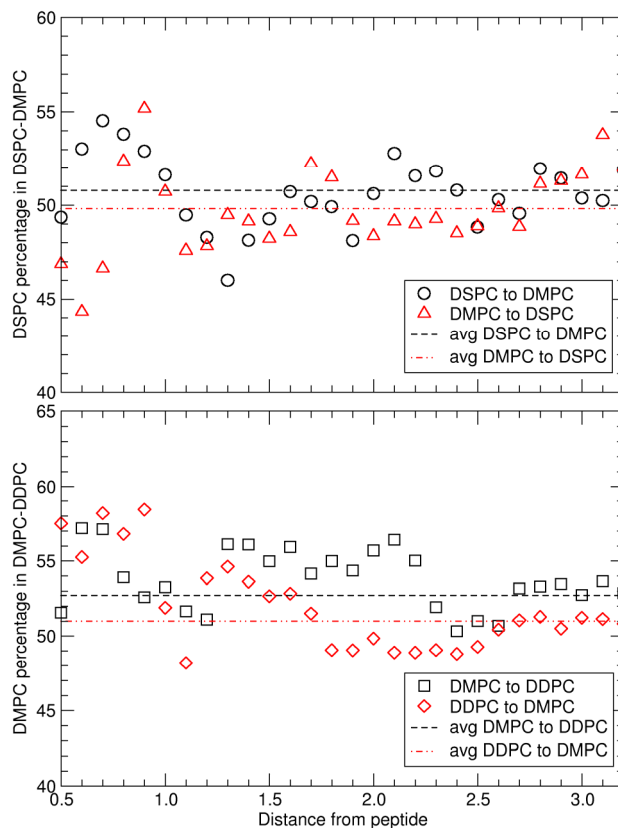


Figure 4.2. Longer lipid composition percentage as radial distance to the center of mass of peptide. Upper panel is the system of DSFC-DMPC/GCA, lower panel is the system of DMPC-DDPC/GCA. Black square are systems mutate from longer lipid, red diamond is systems mutate from shorter lipid.

In the mixed DSFC-DMPC/GCA system, hydrophobic matching is significant as the thickness is up to 0.3 nm less than control value close to peptide and 0.2 nm greater than control value far from peptide. DMPC-DLPC/GCA system has similar trend as the DMPC/GCA system but a steeper thickness decreases as distance increases.

4.4.2 *Hydrophobic Sorting*

Because GCA insertion made a smaller perturbation to the thickness of DMPC bilayers than to DDPC or DSPC bilayers, it provides the best hydrophobic match over all the lipids. We hypothesized that hydrophobic matching should promote enrichment of the DMPC component of DDPC-DMPC or DMPC-DSPC mixtures in the immediate neighborhood of the peptide. The results of the current simulations offer at best weak confirmation of this hypothesis. In Figure 4.2, which shows composition as functions of distance from the peptide center of mass in the plane of the bilayer, the DMPC-DDPC/GCA system (lower panel) shows about 5% of DMPC enrichment close to peptide, in agreement with the hypothesis. In the DSPC-DMPC/GCA system, the lipid composition close to the peptide (within 0.8 nm lateral distance of its center of mass) is not well equilibrated, as indicated by the disagreement between simulations with different starting compositions; if anything, this region appears to be enriched in DSPC. In both trials, the distribution profiles suggest a weak (< 5%) enrichment of DMPC at about 1.2 nm distance that falls off gradually over the next 1-2 nm.

In view of the strong effects of the peptide's presence on bilayer thickness shown in Figure 4.1, the absence of a significant lipid sorting effect is notable. We can infer that the free energy penalty for lipids to accommodate to a range of local bilayer thicknesses is weaker than the entropy of mixing penalty for lipids to rearrange. As has been noted in the context of curved bilayer mixtures^{94,95}, elasticity effects tend to be small enough on a per-lipid basis that they rarely lead to significant demixing unless coupled with an intrinsic tendency to de-mix. Another factor that influences the present results, and may

obscure the effects of hydrophobic matching, is the distribution of lipid headgroups. In contrast to transmembrane helical peptides with hydrophilic termini that extend into the solvent, the GCA peptide is essentially all hydrophobic, so the lipid headgroups occupy the space above and below it. Figure 4.3 shows the radial distribution of lipid headgroups and tail groups, where both systems have lipid headgroups density extending over the central axis of the peptide, while the tails are sterically excluded from this region. Furthermore, the peptide is thinnest near the bilayer midplane giving it an “hourglass” shape (Figure 4.4 A). Even if hydrophobic matching effects promote bilayer thinning, a lipid with a tail longer than the monolayer thickness may be needed to allow the headgroup to sit on top of the peptide while the tail extends to make contact with the narrow waist. This conformation is represented by the lipids shown in Figure 4.4 B. Shape considerations may therefore drive an enrichment of long-tail lipids very close to the peptide under both positive and negative mismatch conditions.

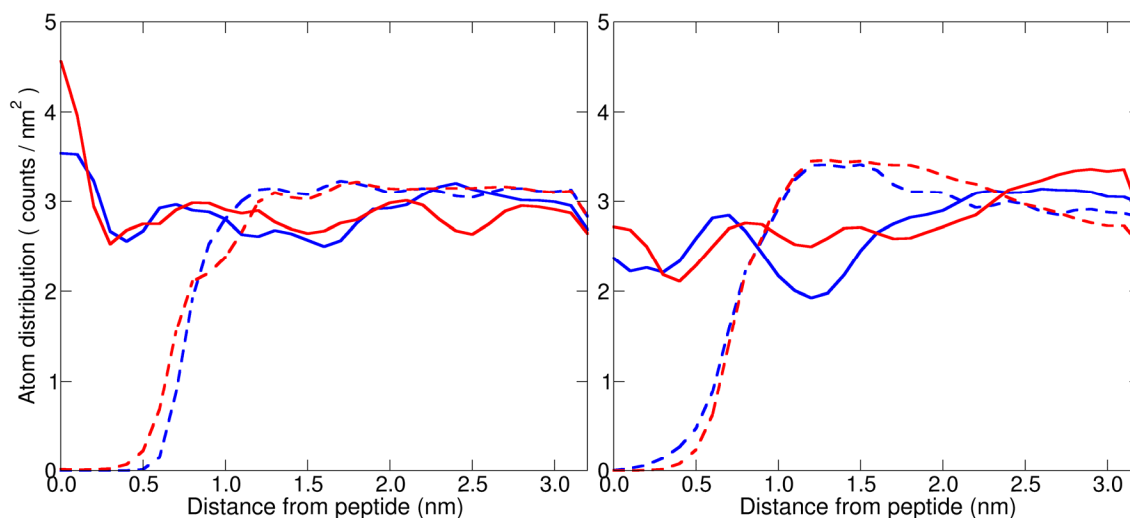


Figure 4.3. Radial distribution of lipid head groups and lipid tail groups from center of peptide. Head groups are shown in solid lines and tail groups are shown in dashed lines. The left panel shows the DSPC-DMPC system, and the right panel shows the DMPC-DDPC system. In each plot, blue lines represent systems mutating lipids, from longer and red lines represent systems mutating from shorter lipids.

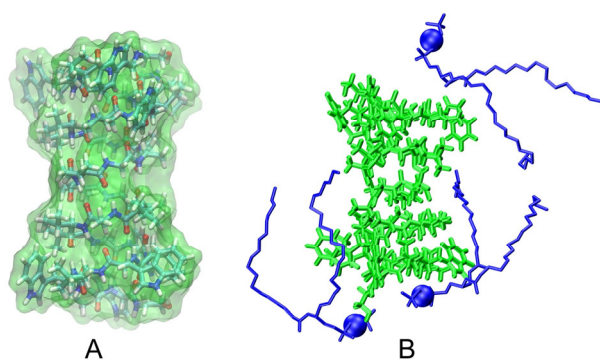


Figure 4.4. Gramicidin A dimer in hourglass shape. (A) the structure of GCA in DMPC, obtained from solid-state NMR⁹². (B) snapshot of DSPC-DMPC/GCA system, where GCA is shown in green, and DSPC on top of GCA is shown in blue (beads represent head groups).

4.4.3 Peptide Tilt

Tilt is an important factor in describing the behavior of transmembrane peptide.

Generally, a high tilt angle with respect to the bilayer normal is favored in positive hydrophobic mismatching case, where peptide may tilt to accommodate bilayer thickness⁴⁶ in addition to lipid stretching. Low tilt angle is more favorable for negative hydrophobic match, where bilayer thinning is the only source for hydrophobic matching.

In Figure 4.5, the evolution of tilt angle for GCA with mixed lipids in MCMD simulations is shown as a function of time. In the present simulated time scale, GCA in DMPC-DDPC mixtures mutated from DMPC or DDPC have similar tilt angle distribution average ($25^{\circ}\pm 8^{\circ}$ and $25^{\circ}\pm 7^{\circ}$). However, GCA in DSPC-DMPC mixtures has broad separation of tilt angles between two configurations. For system started with all DMPC, tilt angle is $26^{\circ}\pm 4^{\circ}$; and system started with all DSPC, tilt angle is $7^{\circ}\pm 8^{\circ}$.

Previous studies on WALP peptide indicates that the embedded peptide, in the case it has longer hydrophobic length than the bilayer hydrophobic thickness, may take 10 ns to tilt to the optimal angle to reduce hydrophobic mismatch⁸⁷. The rate of angle fluctuations may limit the convergence rate for composition fluctuations, providing an explanation for the poorer composition convergence in the DSPC-DMPC mixtures.

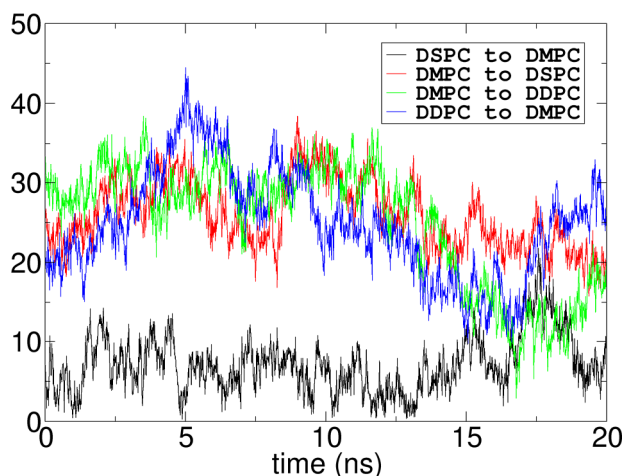


Figure 4.5. GCA tilt angle (parallel to z axis is 0 degree) in the second part of MCMD (black DSPC to DMPC, red DMPC to DSPC, green DMPC to DDPC, blue DDPC to DMPC).

4.5 Conclusions

The gramicidin A trans-membrane dimeric helical peptide was simulated in mixed-lipid bilayers with compositions typical of either positive (DDPC-DMPC) or negative (DMPC-DSPC) hydrophobic mismatch conditions. Use of configuration-bias Monte Carlo mutation moves within the semi-grand canonical ensemble allowed the lateral distribution of long-tail and short-tail lipids to be equilibrated to within roughly $\pm 3\%$. Lipid sorting followed the expected trend in the case of positive hydrophobic mismatch, with the longer-tail DMPC lipid weakly enriched (by about 5%) near the peptide. In the negative hydrophobic mismatch regime, the expected trend of short-tail lipid content increasing near the peptide was at most very weakly present from 3 nm to 1.2 nm lateral distance from the peptide center axis, while the counterintuitive reverse trend appeared at yet shorter distances. A possible explanation for this reverse trend is that longer-tail

lipids are better able to adhere to the hourglass-shaped contours of the GCA helix. A general conclusion is that even in cases of significant perturbations to bilayer thickness, the degree of lateral redistribution of lipids differing in tail length by four carbons is not dramatic, so that it lies nearly within the random fluctuations even when the MCMD scheme is used to accelerate the equilibration of lipid lateral distribution. Furthermore, the details of peptide shape, and not only the hydrophobic length, might have a significant influence on the composition of lipids in close contact with a peptide.

5 Simulations of Lipid Sorting Effects near Beta Barrel Peptide with Atomistic Model and Coarse Grained Model

5.1 Abstract

To understand effects of lipid composition on membrane protein function in a complex mixture like a biomembrane requires knowledge of whether lipid composition local to the protein differs from the mean lipid composition. Atomistic simulations within a semi-grand canonical ensemble have been performed to achieve an equilibrated lateral distribution of long- and short-tailed lipids in mixed-lipid bilayers containing a beta-barrel peptide, OmpA transmembrane domain. Investigations have been performed on beta-barrel peptide embedded in binary mixtures of lipids that differ in tail length. Comparisons between equilibrium lateral distributions obtained using an atomistic model versus a coarse-grained model suggest a strong sorting effect.

5.2 Introduction

Biological membranes are complex and highly organized multiple component assemblies composed of a large variety of lipids, protein, and other molecules. In the conventional picture, fluid lipid bilayer assures the lateral mobility of the embedded components to support biological functions. The hydrophobic interaction between the lipid acyl chains and the protein transmembrane span is one of the most important factors in the membrane self-assembly process, which leads to the heterogeneity of the membrane⁹⁶. The “hydrophobic matching” concept has been introduced to explain the lateral distributions

of these various molecular species, due to its simplicity and elegance to qualitatively interpret the protein lipid interplay. The matching of the hydrophobic surface of proteins by the acyl chains of the lipids is energetically more stable, so the lipids with higher flexibility and mobility tend to adjust their acyl chain order to accommodate the protein transmembrane portion by resizing the hydrophobic thickness of bilayer. Theoretical, experimental, and computational studies^{29,53} have been performed to validate the concept, and distinct characteristics of the outcomes are exhibited. If the hydrophobic length of the transmembrane span is significantly longer than the bilayer thickness, a local bilayer stretching will occur, referring as “positive mismatch”. If the hydrophobic length of the transmembrane span is significantly shorter than the bilayer thickness, a local bilayer compress will occur, referring as “negative mismatch”. No noticeable bilayer thickness perturbation would be found if the hydrophobic lengths of the two moieties are matched. Significant thickness variations are commonly associated with curvature effects, and this interplay can lead to long-range attractions between peptides⁹⁰ and non-monotonic relaxation of thickness vs. distance from the perturbing peptide⁶⁶.

In a bilayer consisting of more than one lipid components with different hydrophobic lengths, lipid sorting or reorganization may accommodate the hydrophobic length of the transmembrane peptide³⁰, in addition to stretching or shrinking the bilayer local thickness. Several experiment results demonstrated the protein/lipid sorting in membranes from different aspects. Dumas et al.⁴⁸ used fluorescence energy transfer method to measure lipid sorting effect in the mixture of DLPC and DSPC with integral bacteriorhodopsin (BR) peptide. Clear association between BR and DLPC-rich domains are observed in gel-

gel and gel-fluid coexistence regimes at 263 K and 293 K. Although MC simulations predicted that BR still prefers to associate with DLPC in the fluid phase mixture, experiment at 338 K is unable to distinguish any association difference. Fahsel et al.⁹¹ used DMPC and DSPC with integral gramicidin to study the lateral membrane organization and phase behavior by neutron scattering, infrared spectroscopy and fluorescence microscopy, and found a preference for the DMPC-rich phase in the mixture under both gel-fluid and gel-gel coexistence conditions. Ridder et al.⁵³ applied a photo-crosslinking study to the WALP23 helical peptide within several mixtures of longer and shorter tailed lipids (including DLPC-DSPC). By analyzing lipid types bonded to the peptide, they found sorting effect is significant in the two-phase region but undetectable in homogeneous fluid-phase mixtures.

Due to the slow lateral diffusion rate of lipid in bilayers, the computational expense of atomistic simulations makes it nearly prohibitive to perform molecular dynamics simulations long enough for a mixture of lipids to reach equilibrium. However, Coarse-Grained (CG) model overcomes the limit by using less number of particles and longer MD integration steps, and thus increases lipid diffusion rate. Klein et al.⁵⁵ simulated the sorting of peptide in mixed lipids with CG model. A van de Waals model cylinder, which consists of hydrophobic sites capped with hydrophilic ends with 15 Å in radius and 20 Å long, was used to represent a transmembrane peptide. Enrichment of short lipid, which matches the peptide, was observed after 1 ns of MD simulation. Sansom et al.⁵⁶ systematically studied the distribution of lipid in two component lipid bilayers with the perturbation of a set of peptides, including generalized alpha helical bundle and beta

barrel. A series of CG-MD simulations of generalized α -helix bundle in three systems for 3 μ s clearly shows that the hydrophobic length preferred lipid is more abundant in the first shell around the peptide.

In order to overcome the limit of conventional MD method in studying lipid sorting, we use a hybrid Monte Carlo-molecular dynamics (MC-MD) approach that allows mutations between long and short-tailed lipids by attempting configurational bias Monte Carlo mutation moves within the isomolar semi-grand canonical ensemble (fixed total number of lipids, a specified difference in chemical potential $\Delta\mu$ between two lipid components, the number of solvent and any other components, pressure, surface tension, and temperature⁵⁹). In a system containing a peptide embedded in a lipid bilayer, the distribution of different types of lipid as a function of distance from the peptide can be monitored over the course of a simulation in which the lipids are undergoing mutation moves. As all lipids in the system are coupled to the same virtual reservoirs of the two components, the distribution of the two lipid types throughout the system converges to an equilibrium lateral distribution with respect to the exchange of any pair of lipids. Simulation of the same lipid mixture at the same activity ratio in the absence of peptide provides a reference composition at “infinite distance”, so that even if a protein perturbs the local composition over an area greater than the simulation box, a preference for one or the other kind of lipid can be detected. In our previous study⁹⁷, this technique has been applied on Gramicidin-A peptide with DMPC-DDPC and DSPC-DMPC mixed lipid bilayers. Though hydrophobic matching effect is obvious from the simulations, significant hydrophobic sorting is not evident. Several physical properties of the peptide

have been considered that interfere the hydrophobic sorting, including the non-cylindrical shape, small diameter, and fast tilting rate of the peptide.

In the present study, the outer membrane protein A of *Escherichia coli* transmembrane domain (OmpA) is studied in mixed lipid bilayers. The OmpA transmembrane domain consists of residues 1-171, and its high resolution structure in association with *n*-octyltetraoxyethylene (C₈E₄) detergent has been determined by X-ray diffraction analysis⁹⁸, to a resolution of 2.5 Å. It consists of a 2.8 nm diameter regular eight-stranded β -barrel, which is filled with water and exists stably in the fluid phase of lipid bilayers. The longitudinal position of OmpA can be further deduced from the residues from the β -barrel surface⁹⁹. In our work, both Coarse-Grained model and atomistic model were used to simulate the interaction of this peptide with mixed lipid bilayers.

5.3 Methods

5.3.1 Coarse-grained model simulations

Conventional MD simulations on coarse-grained model is performed using Gromacs-4.0.3¹⁰⁰. The MARTINI forcefield for lipid and protein¹⁰¹⁻¹⁰³ is used for Coarse-Grained studies. With the unified particle mass in the CG simulation, the MD integration time step is set to 25 fs with temperature of 323 K. The elastic network model¹⁰⁴ is applied to OmpA to suppress the peptide shape deformation in the long time scale simulation. The periodic boundary conditions are applied in three dimensions, with semi-isotropic pressure coupling using the Berendsen barostat algorithm³⁷ at 1 bar at a coupling constant of 1.0 ps and a compressibility of 1×10^{-4} bar. We chose three CG lipid species, CG5,

CG4, CG3 (approximates DSPC, DMPC, DDPC), which consist of the same phosphatidylcholine (PC) head group and 3, 4, 5 CG fatty acyl chain beads, respectively. In each system size, five lipid environments are studied, including pure CG5, pure CG4, pure CG3, 1:1 mixture of CG5-CG4 and CG4-CG3. Lipid bilayer is engineered by duplicating a pair of lipid at tail-to-tail configuration on the lateral directions. After inserting the OmpA peptide in the middle of the engineered pure bilayer, the overlapped lipid pairs are removed and the squared box with OmpA in the middle is obtained. Water is added by using the Gromacs *genbox* tool. Two systems at different sizes are prepared: the large system consists of 1 OmpA, 558 lipids, and 11581 CG water; the small system consists of 1 OmpA, 200 lipids, and 1500 CG water. Self assembly simulation was performed to obtain equilibrated structure. The mixed system is obtained from the pure system by randomly changing half of CG5 to CG4 for CG5-CG4 mixture (or CG4 to CG3 for CG4-CG3 mixture) on each lipid monolayer. An equilibrating simulation was performed to eliminate the vacancy from the particle removal. Started with the initial structure, 1000 ns conventional MD simulation is performed for each system. Due to the slow diffusion rate of lipid, especial in the area near the peptide, the simulation time for mixed lipid system is extended to 2000 ns to allow lipid to fully exchange between the first and outer shell around the peptide.

5.3.2 *Atomistic model simulations*

While Coarse Grained model may explore longer time-scales and larger length-scales, the lack of details in atomistic interactions limits its use in many aspects. In order to regain the atomistic structure from an equilibrated structure given by CG simulation, the reverse

transformation is performed by using the customized Gromacs package developed by Marrink et al.¹⁰⁵ In the transformation, a many-to-one particle mapping was generated for each molecule type, namely the peptide and lipid in this system. In the present configuration, the DDPC, DMPC, DSPC lipids, which have 10, 14, 18 carbons on their each acyl tail, are modeled by CG3, CG4, CG5, respectively. The atomistic topology files are added with an additional “mapping” section, which defines CG particle to atomistic particles in the CG index. The CG water represents 4 SPC water in MARTINI forcefield, so a special 4 water cluster with harmonic constraints on oxygen atoms as one molecule is constructed. An imaginary atomistic structure is created from the CG structure by a script from the same package. The reverse transformation starts with the constructed atomistic structure, and the program with two new functions is able to fit the atomistic particle to the optimized position with restraints to CG particle position.

Gromacs-4.0.3 is used for conventional MD simulations. On atomistic model the combination of protein OPLS-AA (All Atom) forcefield⁷⁴ with united atom lipid forcefield of Berger et al.⁷⁵ is used as suggested by Tieleman et al.⁷⁶ The TIP3P model⁷⁷ of water is used for all simulations. The Langevin thermostat⁷⁸, with a time constant of 0.1 ps, is used to maintain a constant temperature of 330 K in all simulations. The Berendsen barostat⁷⁹ is used for semi-isotropic pressure scaling (at 1 bar pressure, zero surface tension, and time constant of 1.0 ps at assumed compressibility $4.5 \times 10^{-5} \text{ bar}^{-1}$) and the particle-mesh Ewald method for electrostatic forces calculated during the MD step⁸⁰. A time step of 2 fs is used, and the SETTLE⁸¹ and LINCS⁸² algorithms are used to constrain all bonds to fixed lengths.

5.3.3 *Mixed Monte Carlo/MD simulations*

MCMD simulations are performed according to the method in our group recent publication⁵⁹ using GIMLi 1.0, a customized version of Gromacs 3.3, to study the two component lipid bilayer with embedded peptide. A constant ratio of thermodynamic activities (i.e., fugacities) of the two lipid components is used to control the composition of lipids. The activity ratio α can be represented in terms of the chemical potential difference as $\alpha = \exp(\Delta\mu/k_B T)$, where $\Delta\mu = \mu_{\text{DSPC}} - \mu_{\text{DMPC}}$ (or $\mu_{\text{DMPC}} - \mu_{\text{DDPC}}$). During MCMD simulations, after every MD time step, a lipid (e.g. DSPC or DMPC for DSPC-DMPC system) is randomly chosen and subjected to a mutation move attempt using the configuration-bias algorithm⁶⁴. The average success rate is about 0.4% or 1 lipid mutation event in the system on average every 0.5 ps.

5.3.4 *Thickness Analysis*

In both CG and atomistic models, bilayer thickness and lipid distribution are measured as a function of distance from center of mass of the peptide. The reference atom to measure the thickness and distribution were the same: NC3 particle in CG model, and P atom of the headgroup in atomistic model. The radius interval was 0.1 nm. The counts of particles and average position were summed over each interval and all time frames, divided by the number of frames and normalized. Thickness is defined as the z distance between two reference particles at the same radius. Distribution of lipid is defined as the percentage of longer tail lipid in the mixture at the same radius.

5.4 Results and Discussion

5.4.1 Coarsed Grained System

System is presumably equilibrated after 1000 ns MD simulation for the Coarsed Grained system, therefore the 1000-2000 ns trajectory is used for data analysis. As the hydrophobic length of the peptide is approximately equal to tail length of CG3 lipid, and longer than that of CG4 and CG5 lipids, the tilting of peptide would decrease the hydrophobic area exposed to bilayer. Hydrophobic matching effect requires a maximum area contact between the peptide and lipid tails, so OmpA is preferred to stay on its perpendicular orientation, which is also confirmed by visual animation of the trajectory. As a result, the perturbation of the bilayer thickness is dominantly contributed by lipid tail shrinking. Because each CG particle represents several atoms, the simulation results may not be directly comparable to experimental and atomistic simulation results¹⁰³.

Negative hydrophobic matching effects are observed in all simulated systems, and Figure 5.1 shows the bilayer thickness of the systems as a function of the radial distance from the center of the OmpA peptide. Key values of thickness are shown Table 5.1. The thickness of the bilayer, starting at the beta barrel external edge at 1.5 nm, monotonically increases as the distance increase and starts to level off between 3-5 nm depending on the strength of hydrophobic mismatch. Comparing the small and larger systems at the same condition in the present work, the thickness of the small system is slightly higher than that of the large system, indicating a size dependence of the simulation box. Under the periodic boundary condition for lipid bilayer systems, the interactions between repeated images in the bilayer normal direction can be neglected. On the lateral direction, however, lipid bilayer is seamlessly connected between the boundaries, so that the perturbation to

the bilayer in the present system is contributed not only by the inserted peptide but also by its lateral periodical image. The thickness far away from the peptide should converge to its unperturbed value. In an ideal case that the distance from peptide is long enough, the lipid bilayer may relax from perturbation and resume its thickness to a state without a peptide. The small systems show slightly higher thickness value than the corresponding large systems at all lateral distances, indicating the relaxation range of the bilayer is presumably larger than the box size. The pure CG3 lipid bilayer, whose thickness is least perturbed by the peptide, exhibited about 0.3 nm thickness decrease from the thickness maximum of 3.6 nm at a distance of 3.0 nm from the peptide. The pure CG4 and CG5 bilayers showed local thicknesses near the peptide about 1.0 nm lower than thicknesses of 4.4 nm and 5.1 nm away from the peptide. The 1:1 mixed CG3-CG4 bilayer exhibit similar trend on the thickness, with 3.5 nm thick at $r = 1.5$ and 4.0 nm at $r = 3$. The thickness curve of 1:1 CG4:CG5 mixture also approximately overlaps the average of the thickness curves corresponding to pure CG4 and CG5 systems. (3.8 nm at $r = 1.5$ and 4.3 nm at $r = 5$). Comparing the bilayer thickness differences between the near peptide range and far away range, we found that thickness of 1:1 mixture is approximately the average of the pure lipids at distant range. As the radial distance becomes smaller, the thickness shifts towards the value associated with the shorter lipid. This trend suggests that the shorter lipid is more abundant near the peptide. Moreover, the smoothness of the lines concludes that the preference of a lipid type is continuous, and that demixing into distinct, well-defined domains enriched in one lipid type or the other does not happen.

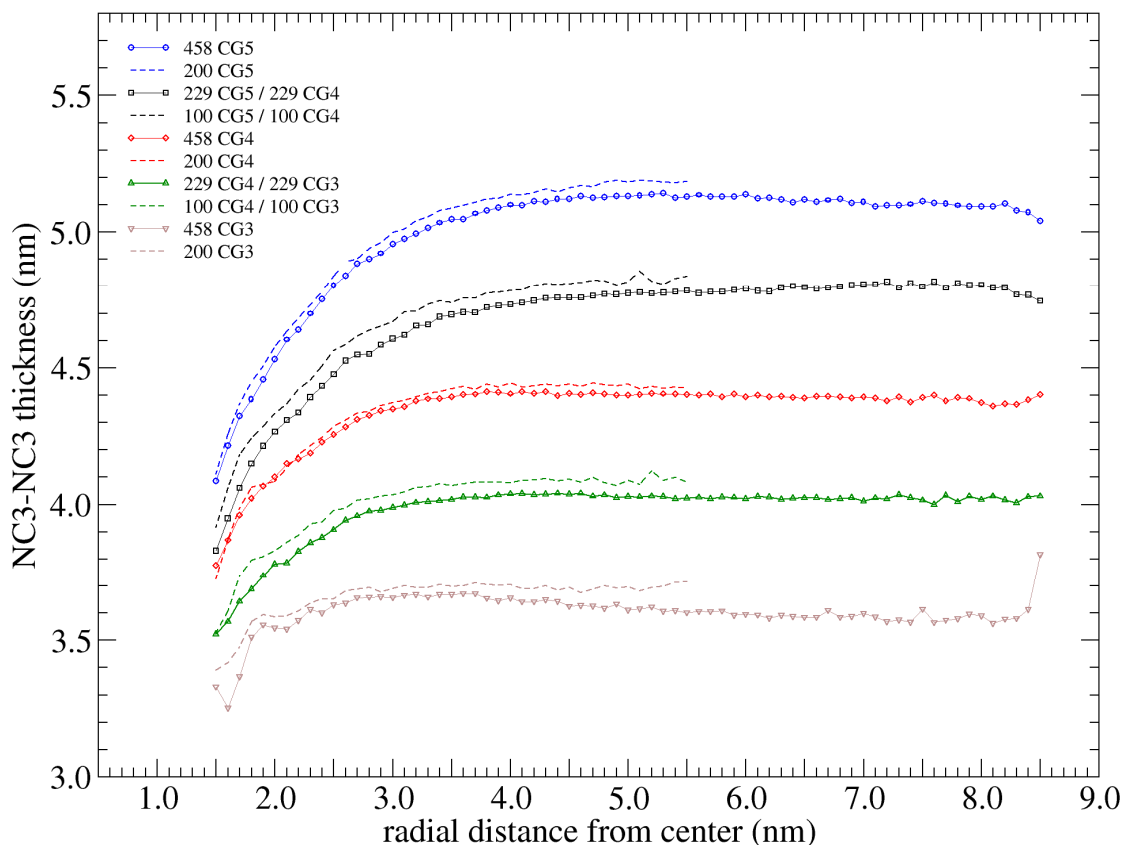


Figure 5.1. Lipid bilayer thickness in Coarse-Grained simulations. Radial interval at 0.1 nm from center of peptide is applied in counting appearance of NC3 particles on each monolayer. The difference of the average z coordinates on each layer at the same radial distance represents the bilayer thickness. From top to bottom, blue, black, red, green, brown colors represent CG5, CG5-CG4, CG4, CG4-CG3, CG3 systems, respectively. Symbols connected with solid lines in the same color represent large systems containing 558 lipids. Dash lines represent small systems containing 200 lipids.

Table 5.1. Bilayer thickness of the peptide embedded coarse grained systems.

Lipid composition	NC3-NC3 lipid bilayer thickness (nm)		
	$r = 1.5$ nm	$r = 3.0$ nm	$r = 5.0$ nm
CG3	3.3	3.6	3.6
CG3-CG4	3.5	4.0	4.0
CG4	3.8	4.3	4.3
CG4-CG5	3.8	4.5	4.8
CG5	4.1	4.9	5.1

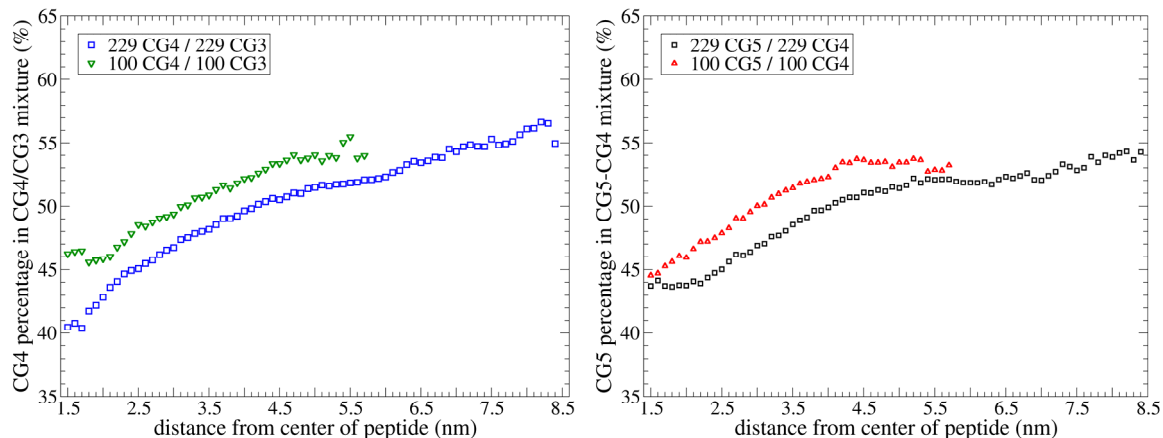


Figure 5.2. Lipid identity radial distribution of 1000-2000 ns Coarse-Grained simulations.

Figure 5.2 shows the radial distribution of lipids of the mixtures. Strong sorting effect of lipid was observed for both mixtures, including small and large systems. The small CG3-CG4 system shows nearly linear percentage increase from 45% at 1.5 nm to 55% at 5.5 nm for the longer lipid (CG4), indicating that the better hydrophobic matched shorter lipid (CG3) prefers to enrich near the OmpA peptide. The large system, in which the radial distance expands to 8.5 nm, also exhibit linear concentration increase of CG4 from 40% to 57% at the box edge. Stronger bilayer thickness perturbation of the longer tail lipids and their mixtures were noted in studying hydrophobic matching effects; however, the degree of sorting is no greater, or in the case of the larger system slightly weaker, suggesting that longer tail lipids can achieve greater variation in local thickness. On the right panel, at 1.5 nm CG4 was 45%, and this number increased to 54% at the edge of both small and large systems. The lower degree of sorting in CG4-CG5 system may be caused by the fact that longer tails have a greater thickness compressibility due to their increased conformational freedom, and so CG4 and CG5 are more interchangeable within different local thickness environments than are CG3 and CG4.

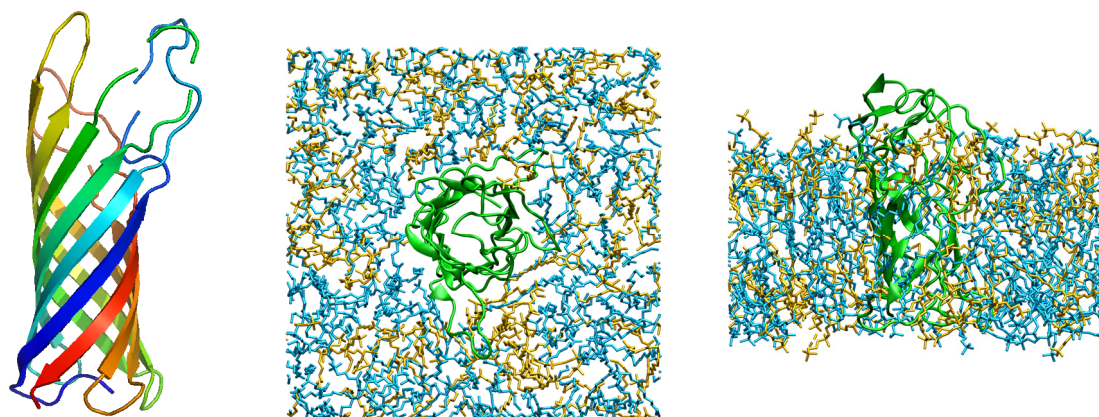


Figure 5.3. Snapshots of OmpA in crystal state and embedded in bilayer. **(a)** Crystal structure of OmpA in cartoon display; **(b)** top view of OmpA embedded in DMPC-DDPC mixture; **(c)** side view of OmpA embedded in DMPC-DDPC mixture.

5.4.2 Atomistic System

Coarse Grained model provides a good prediction of peptide orientation and lipid distribution, including perpendicular position of peptide inside bilayer and distribution pattern of lipids, and the atomistic model obtained from the reverse transformation is considered as an appropriate approach for starting atomistic MD simulations for our current studies. In this study, due to the computational cost of MCMD method, we use smaller atomistic systems containing 128 lipids. These systems are constructed in the same way as the 200 lipid system, and they are simulated for 1000 ns at the same condition for five different lipid compositions. After reverse transformation, systems consisting of pure DSPC, DMPC, DDPC, and mixed half-half DSPC-DMPC and DMPC-DDPC are obtained. Figure 5.3 shows the snapshots of the simulated β -barrel peptide and the peptide embedded DMPC-DDPC lipid bilayer. The mixed systems containing the same number of long and short lipids on each layer are referred as CG DSPC-DMPC (or

CG DMPC-DDPC) in later discussion. Though the transformed structures are good predictions of possible atomistic structure, the constraint simulate annealing may not eliminate possible bad contacts between neighbor atoms, and the obtained structure may also be far from equilibrated state. Conventional MD simulations starting from the transformed structure are performed in 60 ns time scale, and only the 40-60 ns portion is used for analysis. In Figure 5.4 negative hydrophobic mismatch is found in all systems, in agreement with CG models. Pure DDPC system shows a less than 0.2 nm weak thickness change near OmpA, and 0.1 nm thickness increases above the system average. Thickness increase trend along a radius is also found in the DMPC-DDPC mixture, but an anomalous steep thickness increase is observed near the peptide. Visual examination indicates a strong bilayer distortion remains during the simulation, and it is not an equilibrated structure and then should be replaced by another simulation starting at different configuration. DMPC, DMPC-DSPC mixture, and DSPC recognize negative hydrophobic matching, with overall thickness increase from peptide to edge. Thickness in DMPC/peptide system, (3.4 nm thick in the absence of peptide), grows from 3.0 nm next to peptide and reaches 3.8 nm at $r = 4.5$ nm. DMPC-DSPC mixture has about 0.4 nm thickness decrease from the control near the peptide, and has 0.7 nm thickness increase at box edge. The thickness of pure DSPC control system is 4.26 nm, which is 0.8 nm greater than the thickness near the peptide, and 0.4 nm less than the edge thickness. In summary, DDPC is the best hydrophobic matched lipid among the three species. As the bilayer thickness increases by adding or switching to longer tail lipid, the smallest thickness also increases and the difference between edge and center becomes larger.

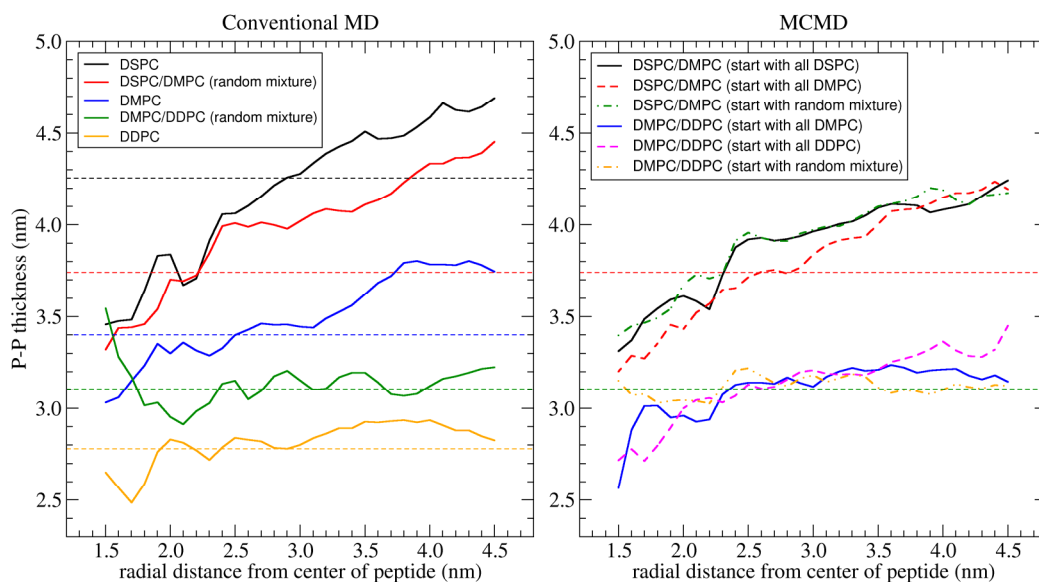


Figure 5.4. Hydrophobic matching of lipids as a function of radial distance from peptide. **(left)** lipid thickness using conventional MD method. Solid lines show the bilayer thickness of each system: black DSPC, red DSPC-DMPC, blue DMPC, green DMPC-DDPC, orange DDPC; dashed lines show the corresponding control system bilayer thickness. **(right)** lipid thickness using MCMD method. Non-horizontal lines represent binary lipid mixtures starting with different compositions. MCMD simulations were performed for DMPC-DDPC mixture and DSPC-DMPC mixture, each has three configurations including starting with 100% lipid type of one component plus a 1:1 CG mixture.

Table 5.2. Average lipid compositions at different starting configurations.

mutation start with	system	Long tail lipids %	Activity ratio
all DMPC	DMPC-DDPC	50.4 ± 0.5	4.00×10^{-4}
all DDPC	DMPC-DDPC	52.4 ± 0.5	4.00×10^{-4}
all DMPC	DMPC-DDPC, OmpA	48.8 ± 0.4	4.00×10^{-4}
all DDPC	DMPC-DDPC, OmpA	48.8 ± 0.4	4.00×10^{-4}
1:1 DMPC:DDPC	DMPC-DDPC, OmpA	50.7 ± 0.6	4.00×10^{-4}
all DSPC	DSPC-DMPC	49.4 ± 0.4	3.87×10^{-4}
all DMPC	DSPC-DMPC	48.4 ± 0.4	3.87×10^{-4}
all DSPC	DSPC-DMPC, OmpA	47.7 ± 0.6	3.87×10^{-4}
all DMPC	DSPC-DMPC, OmpA	45.6 ± 0.7	3.87×10^{-4}
1:1 DSPC:DMPC	DSPC-DMPC, OmpA	47.4 ± 0.7	3.87×10^{-4}

The systems reach equilibrated states in 60 ns conventional MD simulation. MCMD simulations are performed to study the lipid demixing for both lipid mixtures, starting from 100% each type of lipid and the half-half mixture. Because both lipids mutations and lipid/protein rearrangements require sufficient time to reach a new equilibrium, we discard first 20 ns and only use 20 to 40 ns in each trajectory for the following analysis. Control simulations for 20 ns of each mixed lipid layer without peptide have also been performed. Table 5.2 shows the average composition of long-tail lipid in each trajectory. From preliminary MCMD simulations, the activity corresponding to a 1:1 proportion of lipid types is estimated to be 4.00×10^{-4} for DSPC/DMPC and 3.87×10^{-4} for DMPC/DDPC. Uncertainty for each trajectory is calculated using the method of Wang et al⁶¹ (equation 2). In all three DMPC-DDPC/OmpA systems the DMPC percentage is smaller: the difference varies from 0.7%-2.6% comparing with the control average 51.4%. The DMPC percentage starting with all DMPC or DDPC is 48.8%, which is 2.6% lower than the control. Starting with the 1:1 DMPC-DDPC mixture converted from CG simulation trajectory ending structure, the DMPC percentage is 50.7%, which is 1.9% higher than the other two systems, but still lower than the control result. In the DSPC-DMPC mixture, the average DSPC percentage of control systems is 48.9%. With embedded OmpA peptide the DMPC percentage varying from 45.6% to 47.7%, which is 1.2%-3.3% lower. The lipid ratio has not perfectly converged to the range counting the uncertainty, and longer simulation may be needed to obtain better statistics. The control simulation represents the bilayer at infinite distance from peptide, so in the peptide embedded simulations the increased percentage of short tail lipid at equilibrium indicates a preference of shorter tail lipids to occupy the sites near the peptide resulting from the

chemical potential difference. The greater difference between systems with peptide and without peptide reflects the theory that the free energy change is proportional to the square of hydrophobic mismatch length.

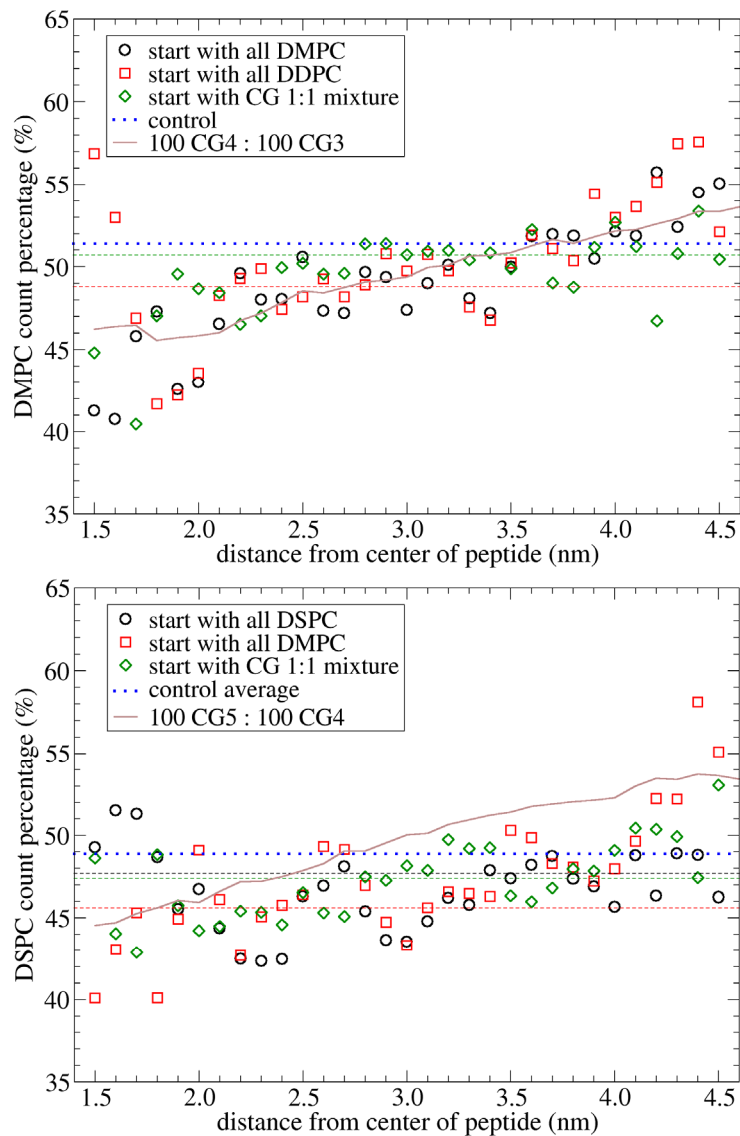


Figure 5.5. (upper) Lipid radial distribution for DMPC-DDPC mixture. Horizontal dashed lines are the average of lipid percentage for corresponding systems of the same color: black 48.8%, red 48.8%, green 50.7%. Blue dotted line is the average of control system, 51.4%. Brown solid line is for the 200 lipid CG3/CG4 system. **(lower)** Lipid radial distribution for DSPC-DMPC mixture. Horizontal line values are: black 47.7%, red 45.6%, green 47.4%. Brown solid line is the 200 lipid CG4-CG5 system. Blue dotted line is the average of control system, 48.9%.

The radial distributions of lipid types as a function of distance from the center of OmpA peptide for both mixtures are shown in Figure 5.5. Each mixture is compared with the corresponding small Coarsed Grained system containing 100 long lipids and 100 short lipids. Strong lipid sorting effect is evident. With any starting configuration, the better matched DDPC lipid is favored near the peptide and the DMPC lipid ratio increases as the distance from the peptide increases. The system starting from 1:1 DMPC-DDPC has the lowest DMPC percentage near the peptide, and the system starting from all DMPC or all DDPC has the same higher DMPC percentage. However, the lipid density distribution shows that in the 1.5-1.7 nm distance range the average number of lipid per unit area is smaller than that of the pure lipid bilayer. This would be resulted from the peptide distortion, which changes cylinder shape of the beta barrel and reduces the area occupied by lipids. In another case, the lipid headgroup may have higher chance to bind to the peptide and its tail length can be different than the optimal length. Extending the MCMD simulation length would be able to eliminate the unpredicted observables, and also reduce fluctuations on the distribution curve. Nevertheless, in Figure 5.5 hydrophobic sorting of three atomistic systems matches CG system data, represented by a solid line that crosses the atomistic data points in a similar trend. On the far end from the peptide, enrichment of DMPC is observed, suggesting hydrophobic matching effect confirmed by the fact that DMPC lipid as the mismatched lipid has higher preference to stay at the edge of box. In the DSPC-DMPC/OmpA system, neither lipid is perfectly matched, but the better matched DMPC exhibits higher concentration near the peptide. Similar to the phenomenon of DMPC-DDPC/OmpA, significant fluctuation is found between 1.5-1.8 nm that some data points are higher than the average value. In contrast, DSPC is more

abundant at edge of box. The CG system data as the comparison line is higher than the atomistic trend. However, the ratio of long and short lipids is not perfectly 1:1 in the atomistic simulations. If the degree of hydrophobic sorting keeps the same trend against a small variation of lipid composition, the average lipid percentage should be used as a baseline in comparing degree of sorting for systems that have different lipid ratios. If we calculate the percentage difference between atomistic systems and coarse-grained systems (50%) and shift the coarse-grained line by the same amount in Figure 5.5, we would find that solid line matches the corresponding atomistic system data points.

In order to place the radial distribution function in the context of the radially varying number of neighbors, we calculate the integrated mean excess number⁶² of lipid as a function of radial distance from the center of OmpA peptide (Figure 5.6). The excess number of a given type of lipid is defined as difference between the actual mean number of lipids of that type within a given distance and the number that would exist in a randomly mixed system without peptide at the same activity ratio. In DMPC-DDPC/peptide systems, excess DDPC lipid value increases linearly from approximately 1 nm to 3 nm for starting from all DMPC and all DDPC. The system starting with 1:1 DMPC-DDPC has very small excess lipid value, indicating no strong sorting in this system. In DSPC-DMPC/peptide systems, strong preference of DMPC is found for all starting configurations. In addition to lipid composition shown in table 5.2, this observation confirms the theoretical prediction given by equation 2.1, that the free energy of protein integral system is proportional to the square of hydrophobic mismatch. In this case, the mismatch of DDPC is close to zero, and the mismatch of DSPC is

approximately the twice of DMPC. As a result, the DSPC-DMPC/peptide system exhibits higher degree of hydrophobic sorting.

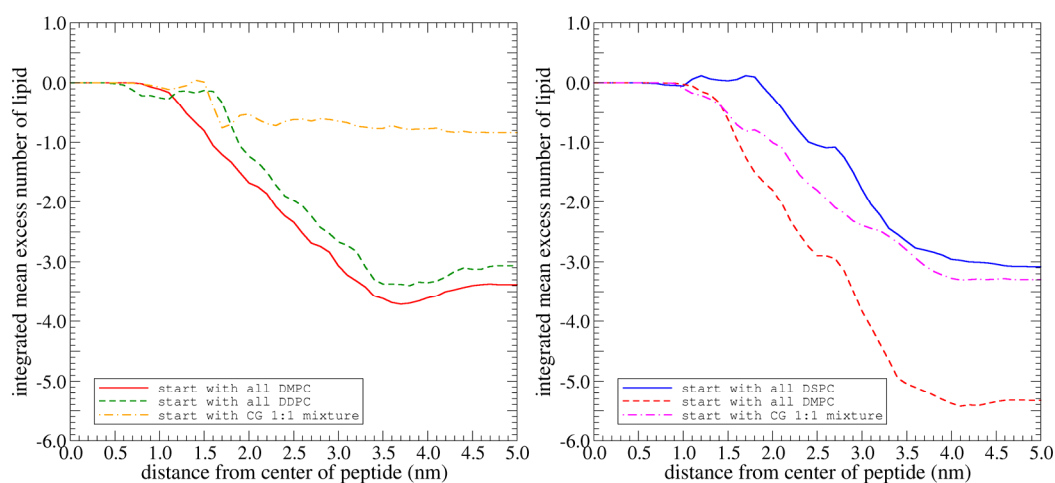


Figure 5.6. Mean excess number of longer tail lipid to the control average versus radial distance from the center of peptide. Left panel represents the DMPC-DDPC/peptide systems, with MCMD mutation starting with all DMPC, DDPC, and 1:1 CG DMPC-DDPC mixture. Positive number indicates excess number of longer tail lipid (DMPC), and negative number indicates excess number of shorter tail lipid (DDPC). Right panel represents the DSPC-DMPC/peptide systems, with MCMD mutation starting with all DSPC, DMPC, and 1:1 CG DSPC-DMPC mixture. Positive number indicates excess number of longer tail lipid (DSPC), and negative number indicates excess number of shorter tail lipid (DMPC).

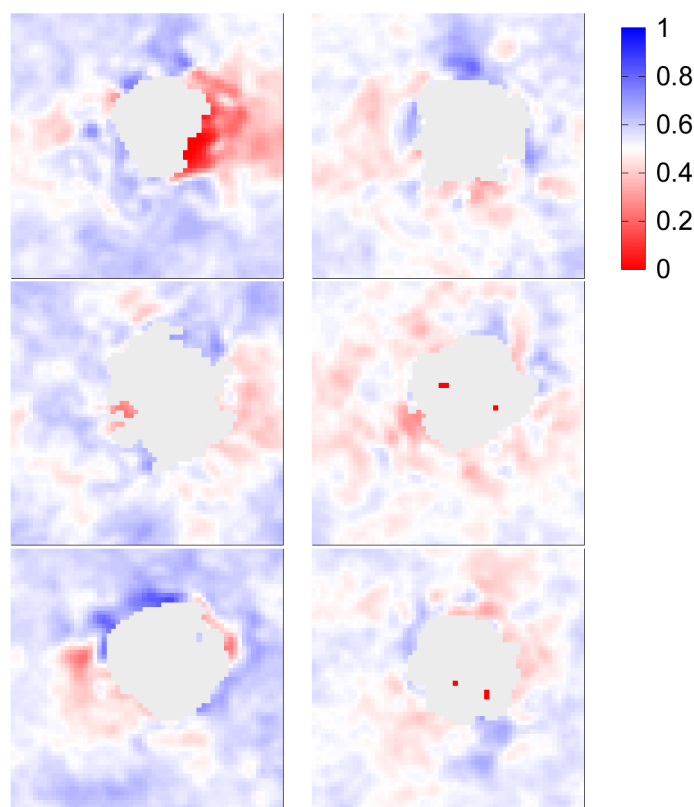


Figure 5.7. Lipid lateral distribution pattern in the mixed lipid bilayer with embedded peptide. Color scale represents fraction of longer-tail lipid (higher fractions in blue). The simulation box on the lateral dimension is $4 \text{ nm} \times 4 \text{ nm}$. The grey block in the center of each plot represents the peptide. Left column represents the DMPC-DDPC/peptide systems, with MCMD mutation starting with all DMPC, DDPC, and CG DMPC-DDPC mixture. Color indicates ratio of longer tail lipid (DMPC) versus all lipids. Right column represents the DSPC-DMPC/peptide systems, with MCMD mutation starting with all DSPC, DMPC, and CG DSPC-DMPC mixture.

Two-dimensional plot of composition (Figure 5.7) shows greater detail of the lateral distribution of lipids in the mixed lipid bilayers with embedded peptide. Lateral grid at 0.1 nm interval is used for binning particles for each lipid type. Grid points with 50% or

fewer particles than the average are dropped. The rotation of the peptide around the bilayer normal is slow in the simulation timescale, so that the peptide is oriented in the same direction in all systems. In all cases, the distribution of the two lipid types is not uniform around the surface of the peptide, but no particular pattern is conserved suggesting that specific sites on the peptide are not determining these fluctuations. The most consistent observation across all runs is that the corners of the simulation box, representing the area farthest from all periodic images of the peptide, are uniformly enriched in the longer-tail lipid.

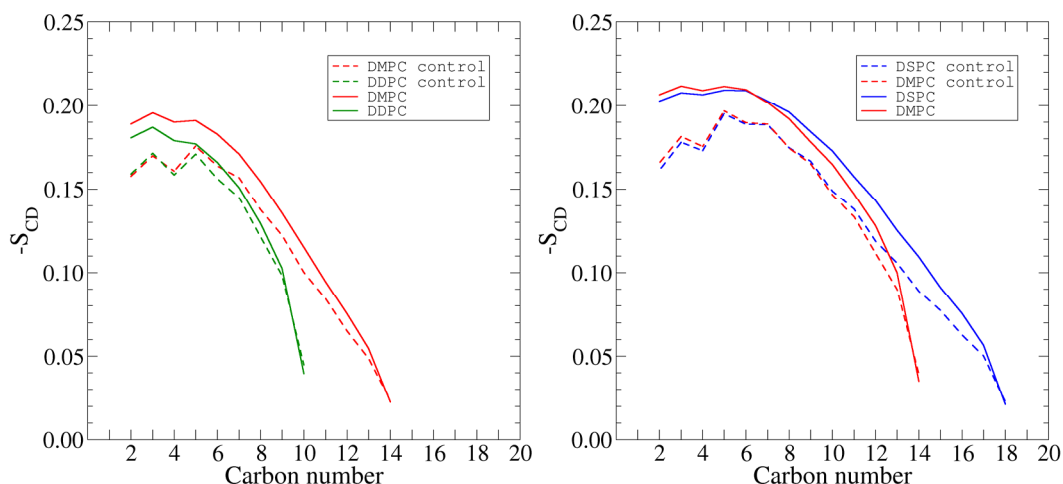


Figure 5.8. Average C-H bond order parameter profile. Solid line shows the average order parameter of lipids with the presence of beta barrel peptide. Dashed line shows the control value. On the left panel, red represents DMPC, and green represents DDPC, for the DMPC-DDPC/peptide mixture. On the right panel, blue represents DSPC, and red represents DMPC, for the DSPC-DMPC/peptide mixture.

The order parameter of C-H bond in the lipid acyl chains for the DMPC-DDPC and DSPC-DMPC mixtures are shown in Figure 5.8. In both systems, the presence of peptide significantly increases the acyl chain order. This result is surprising, given that it is generally expected that the decrease of bilayer thickness is associated with a reduction in order parameters. In the present system, the embedded beta barrel peptide has a cylindrical shape that locally appears to the lipids as a flat wall normal to the bilayer, which due to interfacial packing effects may tend to order the nearby lipids, approximately 10 of which are in direct contact with the peptide for each leaflet. Furthermore, in the DSPC-DMPC/peptide system in particular, the thinning of the bilayer adjacent to the peptide is offset by thickening in the regions farther away; the bilayer thickened area is approximately 75% of the total lipid bilayer area. The maximum thickness of the DMPC-DDPC/peptide system is only marginally thicker than the peptide-free control, but also shows weaker thinning near the peptide.

Tilt is an important factor in describing behavior of peptide in addition to the perturbation of bilayer thickness. Generally, a high tilt angle with respect to the bilayer normal is favored in positive mismatch case, where peptide may tilt to accommodate bilayer thickness⁴⁶ in addition to lipid stretching. Low tilt angle is more favorable for negative hydrophobic mismatch, where bilayer compressing is the only source for hydrophobic matching. In the present study, no noticeable peptide tilt is observed in either CG model or atomistic model, in agreement with the prediction of negative hydrophobic mismatch.

5.5 Conclusions

The OmpA transmembrane domain beta barrel peptide has been simulated in lipid bilayers with atomistic and coarsed-grained models. The Coarse Grained model using 3, 4, 5 particles (CG3, CG4, CG5) shows strong system size dependence on hydrophobic sorting, indicating a system at least as large as 500 lipids is needed to give low-concentration limit. The hydrophobic length of the peptide is slightly smaller than that of the shortest CG3 lipid, and the strength of negative hydrophobic mismatch increases as the lipid thickness increases. Since all lipids in the bilayers have negative hydrophobic mismatch, the shorter tail lipid is energetically more favorable near the peptide in an equilibrated system. Lipid sorting follows the predicted trend for negative hydrophobic mismatch that shorter-tail lipids enrich near the peptide. The degree of sorting for the small system is similar between CG3-CG4 and CG4-CG5 mixtures by comparing the radial distribution of lipids from the embedded peptide. However, in the large system, the CG3-CG4 mixture exhibits higher degree of sorting than does the CG4-CG5 mixture, indicating that at a fixed lipid composition, the long-tail lipid may adapt bilayer thickness changes by adjusting tail lengths in a higher portion.

In atomistic model OmpA peptide is embedded in DMPC-DDPC and DSPC-DMPC lipid bilayers, corresponding to CG4-CG3 and CG5-CG4 lipid bilayers in CG model.

Hydrophobic sorting effects are generally observed from MCMD simulations. In comparison with CG model results, atomistic model gives a qualitative similarity in results, validating that Coarse-Grained method is a suitable method in studying lipid hydrophobic sorting. Moreover, in the atomistic model the degree of sorting by OmpA

peptide is larger with DSPC-DMPC than with DMPC-DDPC, consistent the theoretical prediction of the stronger thinning effect in DSPC-DMPC.

In spite of local thinning, order parameter shows counter-intuitive ordering, that lipids are more ordered than they are not perturbed with transmembrane peptide. Though thinning in lipid bilayer usually induces order parameter decrease, the existence of cylindrical peptide aligns nearby lipids and increases their order significantly.

References

1. von Heijne, G.; Rees, D. Membranes: reading between the lines. *Current Opinion in Structural biology* **2008**, *18*, 403.
2. Singer, S.J.; Nicolson, G.L. The fluid mosaic model of the structure of cell membranes. *Science* **1972**, *175*, 720.
3. Ottolenghi, A. Preparation and characterization of mouse intestinal phospholipase. *Lipids* **1973**, *8*, 415.
4. Israelachvili, J.N. Refinement of the fluid-mosaic model of membrane structure. *Biochimica et Biophysica Acta* **1977**, *469*, 221.
5. Mouritsen, O.G. Theoretical models of phospholipid phase transitions. *Chemistry and Physics of Lipids* **1991**, *57*, 179.
6. Sperotto, M.M.; Mouritsen, O.G. Lipid enrichment and selectivity of integral membrane proteins in two-component lipid bilayers. *European Biophysics Journal* **1993**, *22*, 323.
7. Mouritsen, O. G. Computer simulation of cooperative phenomena in lipid membranes. In *Molecular Description of Biological Membrane Components by Computer Aided Conformational Analysis*; Brasseur, R., Ed.; CRC Press: Boca Raton, FL, **1990**; Vol. 1, p 3.
8. Jørgensen K.; Sperotto M.M.; Mouritsen O.G.; Ipsen J.H.; Zuckermann M.J. Phase equilibria and local structure in binary lipid bilayers. *Biochimica et Biophysica Acta* **1993**, *1152*, 135.

9. Ipsen, J.H.; Jørgensen, K.; Mouritsen, O.G. Density fluctuations in saturated phospholipid bilayers increase as the acyl-chain length decreases. *Biophysical Journal* **1990**, *58*, 1099.
10. Ruggiero, A.; Hudson, B. Critical density fluctuations in lipid bilayers detected by fluorescence lifetime heterogeneity. *Biophysical Journal* **1989**, *55*, 1111.
11. Biltonen, R.L. A statistical-thermodynamic view of cooperative structural changes in phospholipid bilayer membranes: their potential role in biological function. *The Journal of Chemical Thermodynamics*, **1990**, *22*, 1.
12. Freire, E, Biltonen, R. Estimation of molecular averages and equilibrium fluctuations in lipid bilayer systems from the excess heat capacity function. *Biochimica et Biophysica Acta* **1978**, *514*, 54.
13. Andersen, O.S.; Koeppe, R.E. 2nd. Bilayer thickness and membrane protein function: an energetic perspective. *Annual Review of Biophysics and Biomolecular Structure* **2007**, *36*, 107.
14. Edidin, M. The state of lipid rafts: from model membranes to cells. *Annual Review of Biophysics and Biomolecular Structure* **2003**, *32*, 257.
15. Epand, R.M. Cholesterol and the interaction of proteins with membrane domains. *Progress in Lipid Research* **2006**, *45*, 279.
16. Kusumi, A.; Nakada, C.; Ritchie, K.; Murase, K.; Suzuki, K.; Murakoshi, H.; Kasai, R.S.; Kondo, J.; Fujiwara, T. Paradigm shift of the plasma membrane concept from the two-dimensional continuum fluid to the partitioned fluid: high-speed single-molecule tracking of membrane molecules. *Annual Review of Biophysics and Biomolecular Structure* **2005**, *34*, 351.

17. Kusumi, A.; Suzuki, K. Toward understanding the dynamics of membrane-raft-based molecular interactions. *Biochimica et Biophysica Acta* **2005**, *1746*, 234.
18. Simons, K.; Vaz, W.L. Model systems, lipid rafts, and cell membranes. *Annual Review of Biophysics and Biomolecular Structure* **2004**, *33*, 269.
19. Lingwood, D.; Simons, K. Lipid rafts as a membrane-organizing principle. *Science* **2010**, *327*, 46.
20. Simons, K.; Ikonen, E. Functional rafts in cell membranes. *Nature* **1997**, *387*, 569.
21. Chamberlain, L.H.; Burgoyne, R.D.; Gould, G.W. SNARE proteins are highly enriched in lipid rafts in PC12 cells: implications for the spatial control of exocytosis. *Proceedings of the National Academy of Sciences of the United States of America* **2001**, *98*, 5619.
22. Lang, T.; Bruns, D.; Wenzel, D.; Riedel, D.; Holroyd, P.; Thiele, C.; Jahn, R. SNAREs are concentrated in cholesterol-dependent clusters that define docking and fusion sites for exocytosis. *The EMBO Journal* **2001**, *20*, 2202.
23. Bretscher, M.S.; Munro, S. Cholesterol and the Golgi apparatus. *Science* **1993**, *261*, 1280.
24. Kawabuchi, M.; Satomi, Y.; Takao, T.; Shimonishi, Y.; Nada, S.; Nagai, K.; Tarakhovskiy, A.; Okada, M. Transmembrane phosphoprotein Cbp regulates the activities of Src-family tyrosine kinases. *Nature* **2000**, *404*, 999.
25. Moffett, S.; Brown, D.A.; Linder, M.E. Lipid-dependent targeting of G proteins into rafts. *The Journal of Biological Chemistry* **2000**, *275*, 2191.
26. Simons, K.; Toomre, D. Lipid rafts and signal transduction. *Nature Reviews. Molecular Cell Biology* **2000**, *1*, 31.

27. Mouritsen, O.G.; Bloom, M. Mattress model of lipid-protein interactions in membranes. *Biophysical Journal* **1984**, *46*, 141.
28. Gil, T.; Ipsen, J.H.; Mouritsen, O.G.; Sabra, M.C.; Sperotto, M.M.; Zuckermann, M.J. Theoretical analysis of protein organization in lipid membranes. *Biochimica et Biophysica Acta* **1998**, *1376*, 245.
29. Jensen, M.O.; Mouritsen, O.G. Lipids do influence protein function-the hydrophobic matching hypothesis revisited. *Biochimica Et Biophysica Acta-Biomembranes* **2004**, *1666*, 205.
30. Dumas, F.; Lebrun, M. C.; Tocanne, J. F. Is the protein/lipid hydrophobic matching principle relevant to membrane organization and functions? *FEBS Letters* **1999**, *458*, 271.
31. Mouritsen, O.G.; Bloom, M. Models of Lipid-Protein Interactions in Membranes. Annual Review of Biophysics and Biomolecular Structure. *Annual Review of Biophysics & Biomolecular Structure* **1993**, *22*, 145.
32. Killian, J. A. Hydrophobic mismatch between proteins and lipids in membranes. *Biochimica et Biophysica Acta*, 1998, *1376*, 401.
33. Davis, J. H.; Clare, D. M.; Hodges, R. S.; Bloom, M. Interaction of a synthetic amphiphilic polypeptide and lipids in a bilayer structure. *Biochemistry*, **1983**, *22*, 5298.
34. Zhang, Y. P.; Lewis, R. N. A. H.; Henry, G. D.; Sykes, B. D.; Hodges, R. S.; McElhaney, R. N. Peptide models of helical hydrophobic transmembrane segments of membrane proteins. 1. Studies of the conformation, intrabilayer orientation and

- amide hydrogen exchangeability of Ac-K2-(LA)12-K2-amide. *Biochemistry*, **1995**, *34*, 2348.
35. Killian, J. A.; Salemink, I.; De Planque, M. R. R.; Lindblom, G.; Koeppe II, R. E.; Greathouse, D. V. Induction of nonbilayer structures in diacylphosphatidylcholine model membranes by transmembrane α -helical peptides: importance of hydrophobic mismatch and proposed role of tryptophans. *Biochemistry* **1996**, *35*, 1037.
36. Bloom M.; Evans E.; Mouritsen, O.G. Physical properties of the fluid lipid-bilayer component of cell membranes: a perspective. *Quarterly Reviews of Biophysics* **1991**, *24*, 293.
37. de Planque, M. R. R.; Greathouse, D. V.; Koeppe II, R. E.; Schafer, H.; Marsh, D.; Killian, J. A. Influence of lipid/peptide hydrophobic mismatch on the thickness of diacylphosphatidylcholine bilayers. A ^2H NMR and ESR study using designed transmembrane α -helical peptides and gramicidin A. *Biochemistry* **1998**, *37*, 9333.
38. Harroun, T. A.; Heller, W. T.; Weiss, T. M.; Yang, L.; Huang, H. W. Experimental evidence for hydrophobic matching and membrane-mediated interactions in lipid bilayers containing gramicidin. *Biophysical Journal* **1999**, *76*, 937.
39. Olah G.A.; Huang, H.W.; Liu, W.H.; Wu, Y.L. Location of ion binding sites in the gramicidin channel by x-ray diffraction. *Journal of Molecular Biology* **1991**, *218*, 847.
40. Wu, Y.; He, K.; Ludtke, S.J.; Huang, H.W. X-ray diffraction study of lipid bilayer membrane interacting with amphiphilic helical peptides: diphytanoyl

- phosphatidylcholine with alamethicin at low concentrations. *Biophysical Journal* **1995**, *68*, 2361.
41. Weiss, T.M.; van der Wel, P.C.; Killian, J.A.; Koeppe, R.E. 2nd; Huang, H.W. Hydrophobic mismatch between helices and lipid bilayers. *Biophysical Journal* **2003**, *84*, 379.
 42. Bagatolli, L.A. Direct observation of lipid domains in free standing bilayers: from simple to complex lipid mixtures. *Chemistry and Physics of Lipids* **2003**, *122*, 137
 43. Bernardino de la Serna, J.; Perez-Gil, J.; Simonsen, A.C., Bagatolli, L.A.. Cholesterol rules: direct observation of the coexistence of two fluid phases in native pulmonary surfactant membranes at physiological temperatures. *The Journal of Biological Chemistry* **2004**, *279*, 40715.
 44. Sperotto M.M.; Mouritsen O.G. Monte Carlo simulation studies of lipid order parameter profiles near integral membrane proteins. *Biophysical Journal* **1991**, *59*, 261.
 45. Scott, H. L. Modeling the lipid component of membranes. *Current Opinion in Structural Biology* **2002**, *12*, 495.
 46. Petrache, H. I.; Zuckerman, D. M.; Sachs, J. N.; Killian, J. A.; Koeppe, R. E.; Woolf, T. B. Hydrophobic Matching Mechanism Investigated by Molecular Dynamics Simulations. *Langmuir* **2002**, *18*, 1340.
 47. Kim, T.; Im, W. Revisiting hydrophobic mismatch with free energy simulation studies of transmembrane helix tilt and rotation. *Biophysical Journal* **2010**, *99*, 175.

48. Dumas, F.; Sperotto, M. M.; Lebrun, M. C.; Tocanne, J. F.; Mouritsen, O. G. Molecular sorting of lipids by bacteriorhodopsin in dilauroylphosphatidylcholine / distearoylphosphatidylcholine lipid bilayers. *Biophysical Journal* **1997**, *73*, 1940.
49. Lehtonen, J.Y.; Kinnunen, P.K. Evidence for phospholipid microdomain formation in liquid crystalline liposomes reconstituted with Escherichia coli lactose permease. *Biophysical Journal* **1997**, *72*, 1247.
50. O'Keeffe, A.H.; East, J.M.; Lee, A.G. Selectivity in lipid binding to the bacterial outer membrane protein OmpF. *Biophysical Journal* **2000**, *79*, 2066.
51. Williamson, I.M.; Alvis, S.J.; East, J.M.; Lee, A.G. Interactions of phospholipids with the potassium channel KcsA. *Biophysical Journal* **2002**, *83*, 2026.
52. Fernandes, F.; Loura, L.M.; Prieto, M.; Koehorst, R.; Spruijt, R.B.; Hemminga, M.A. Dependence of M13 major coat protein oligomerization and lateral segregation on bilayer composition. *Biophysical Journal* **2003**, *85*, 2430.
53. Ridder, A. N. J. A.; Spelbrink, R. E. J.; Demmers, J. A. A.; Rijkers, D. T. S.; Liskamp, R. M. J.; Brunner, J.; Heck, A. J. R.; de Kruijff, B.; Killian, J. A. Photo-Crosslinking Analysis of Preferential Interactions between a Transmembrane Peptide and Matching Lipids. *Biochemistry* **2004**, *43*, 4482.
54. König, S.; Sackmann, E. Molecular and collective dynamics of lipid bilayers. *Current Opinion in Colloid & Interface Science*, **1996**, *1*, 78.
55. Nielsen, S. O.; Lopez, C. F.; Ivanov, I.; Moore, P. B.; Shelley, J. C.; Klein, M. L. Transmembrane peptide-induced lipid sorting and mechanism of L α -to-inverted phase transition using coarse-grain molecular dynamics. *Biophysical Journal* **2004**, *87*, 2107.

56. Klingelhoefer, J.W.; Carpenter, T.; Sansom, M.S.P. Peptide Nanopores and Lipid Bilayers: Interactions by Coarse-Grained Molecular-Dynamics Simulations. *Biophysical Journal* **2009**, *9*, 3519.
57. Chang, R.; Ayton, G.S.; Voth, G.A. Multiscale coupling of mesoscopic- and atomistic-level lipid bilayer simulations. *The Journal of Chemical Physics* **2005**, *122*, 244716.
58. Lindblom, G.; Orädd, G.; Filippov, A. Lipid lateral diffusion in bilayers with phosphatidylcholine, sphingomyelin and cholesterol. An NMR study of dynamics and lateral phase separation. *Chemistry and physics of lipids* **2006**, *141*, 179.
59. de Joannis, J.; Jiang, Y.; Yin, F.; Kindt, J.T. Equilibrium distributions of dipalmitoyl phosphatidylcholine and dilauroyl phosphatidylcholine in a mixed lipid bilayer: atomistic semigrand canonical ensemble simulations. *Journal of Physical Chemistry B* **2006**, *110*, 25875.
60. Jiang, Y.; Wang, H.; Kindt, J.T. Atomistic Simulations of Bicelle Mixtures. *Biophysical Journal* **2010**, *98*, 2895
61. Wang, H.; de Joannis, J.; Jiang, Y.; Gaulting, J.C.; Albrecht, B.; Yin, F.; Khanna, K.; Kindt, J.T. Bilayer edge and curvature effects on partitioning of lipids by tail length: atomistic simulations. *Biophysical Journal* **2008**, *95*, 2647.
62. Coppock, P. S.; Kindt, J.T. Atomistic simulations of mixed-lipid bilayers in the gel and fluid phases. *Langmuir* **2009**, *25*, 352.
63. de Joannis, J.; Coppock, P. S.; Yin, F.; Mori M.; Zamorano, A.; Kindt, J.T. Atomistic simulation of cholesterol effects on miscibility of saturated and

- unsaturated phospholipids: implications for liquid-ordered/liquid-disordered phase coexistence. *Journal of the American Chemical Society* **2011**, *133*, 3625.
64. Siepmann, J. I.; McDonald, I. R.; Frenkel, D. Configurational-bias Monte Carlo - A new sampling scheme for flexible chains. *Journal of Physics-Condensed Matter* **1992**, *4*, 679.
65. Lindahl, E.; Hess, B.; van der Spoel, D. GROMACS 3.0: a package for molecular simulation and trajectory analysis. *Journal of Molecular Modeling* **2001**, *7*, 306.
66. Brannigan, G.; Brown, F. L. H. A consistent model for thermal fluctuations and protein-induced deformations in lipid bilayers. *Biophysical Journal* **2006**, *90*, 1501.
67. Venturoli, M.; Sperotto, M. M.; Kranenburg, M.; Smit, B. Mesoscopic models of biological membranes. *Physics Reports-Review Section of Physics Letters* **2006**, *437*, 1.
68. Kandasamy, S. K.; Larson, R. G. Molecular dynamics simulations of model transmembrane peptides in lipid bilayers: a systematic investigation of hydrophobic mismatch. *Biophysical Journal* **2006**, *90*, 2326.
69. Bargmann, C. I.; Hung, M. C.; Weinberg, R. A. Multiple independent activations of the neu oncogene by a point mutation altering the transmembrane domain of p185. *Cell* **1986**, *45*, 649.
70. Aller, P.; Voiry, L.; Garnier, N.; Genest, M. Molecular dynamics (MD) investigations of preformed structures of the transmembrane domain of the oncogenic Neu receptor dimer in a DMPC bilayer. *Biopolymers* **2005**, *77*, 184.

71. van der Ende, B. M.; Sharom, F. J.; Davis, J. H. The transmembrane domain of Neu in a lipid bilayer: molecular dynamics simulations. *European Biophysics Journal* **2004**, *33*, 596.
72. Garnier, N.; Crouzy, S.; Genest, M. Molecular dynamics simulations of the transmembrane domain of the oncogenic ErbB2 receptor dimer in a DMPC bilayer. *Journal of Biomolecular Structure & Dynamics* **2003**, *21*, 179.
73. Khemtouri, L.; Buchoux, S.; Aussenac, F.; Dufourc, E. J. Dimerization of Neu/Erb2 transmembrane domain is controlled by membrane curvature. *European Biophysics Journal with Biophysics Letters* **2007**, *36*, 107.
74. Jorgensen, W. L.; Tirado-Rives, J. The OPLS [optimized potentials for liquid simulations] potential functions for proteins, energy minimizations for crystals of cyclic peptides and crambin. *Journal of the American Chemical Society* **1988**, *110*, 1657.
75. Berger, O.; Edholm, O.; Jahnig, F. Molecular dynamics simulations of a fluid bilayer of dipalmitoylphosphatidylcholine at full hydration, constant pressure, and constant temperature. *Biophysical Journal* **1997**, *72*, 2002.
76. Tieleman, D. P. Membrane protein simulations with a united-atom lipid and all-atom protein model: lipid-protein interactions, side chain transfer free energies and model proteins. *Journal of Physics-Condensed Matter* **2006**, *18*, S1221.
77. Jorgensen, W. L.; Chandrasekhar, J.; Madura, J. D.; Impey, R. W.; Klein, M. L. Comparison of Simple Potential Functions for Simulating Liquid Water. *Journal of Chemical Physics* **1983**, *79*, 926.

78. van Gunsteren, W. F.; Berendsen, H. J. C. A leap-frog algorithm for stochastic dynamics. *Molecular Simulation* **1988**, *1*, 173.
79. Berendsen, H. J. C.; van der Spoel, D.; van Drunen, R. Gromacs - a Message-Passing Parallel Molecular-Dynamics Implementation. *Computer Physics Communications* **1995**, *91*, 43.
80. Ulrich, E.; Lalith, P.; Max, L. B.; Tom, D.; Hsing, L.; Lee, G. P. A smooth particle mesh Ewald method. *Journal of Chemical Physics* **1995**, *103*, 8577.
81. Miyamoto, S.; Kollman, P. A. Settle - an Analytical Version of the Shake and Rattle Algorithm for Rigid Water Models. *Journal of Computational Chemistry* **1992**, *13*, 952.
82. Hess, B.; Bekker, H.; Berendsen, H. J. C.; Fraaije, J. LINCS: A linear constraint solver for molecular simulations. *Journal of Computational Chemistry* **1997**, *18*, 1463.
83. Goetz, M.; Carlotti, C.; Bontems, F.; Dufourc, E. J. Evidence for an alpha-helix -> pi-bulge helicity modulation for the neu/erbB-2 membrane-spanning segment. A H-1 NMR and circular dichroism study. *Biochemistry* **2001**, *40*, 6534.
84. Soumana, O. S.; Aller, P.; Garnier, N.; Genest, M. Transmembrane peptides from tyrosine kinase receptor. Mutation-related behavior in a lipid bilayer investigated by molecular dynamics simulations. *Journal of Biomolecular Structure & Dynamics* **2005**, *23*, 91.
85. Humphrey, W.; Dalke, A.; Schulten, K. VMD: Visual molecular dynamics. *Journal of Molecular Graphics*. **1996**, *14*, 33.

86. Lu, D. L.; Vavasour, I.; Morrow, M. R. Smoothed Acyl-Chain Orientational Order-Parameter Profiles in Dimyristoylphosphatidylcholine-Distearoylphosphatidylcholine Mixtures - a H-2-Nmr Study. *Biophysical Journal* **1995**, *68*, 574.
87. Ozdirekcan, S.; Etchebest, C.; Killian, J. A.; Fuchs, P. F. J. On the orientation of a designed transmembrane peptide: Toward the right tilt angle? *Journal of the American Chemical Society* **2007**, *129*, 15174.
88. de Planque, M. R.; Kruijtz J.A.; Liskamp R.M.; Marsh, D.; Greathouse, D.V.; Koeppe R.E. 2nd; de Kruijff B; Killian J.A. Different membrane anchoring positions of tryptophan and lysine in synthetic transmembrane alpha-helical peptides. *The Journal of Biological Chemistry* **1999**, *274*, 20839
89. de Planque, M. R. R.; Killian, J. A. Protein-lipid interactions studied with designed transmembrane peptides: role of hydrophobic matching and interfacial anchoring. *Molecular Membrane Biology* **2003**, *20*, 271.
90. Botelho, A. V.; Huber, T.; Sakmar, T. P.; Brown, M. F. Curvature and hydrophobic forces drive oligomerization and modulate activity of rhodopsin in membranes. *Biophysical Journal* **2006**, *91*, 4464.
91. Fahsel, S.; Pospiech, E. M.; Zein, M.; Hazlet, T. L.; Gratton, E.; Winter, R. Modulation of concentration fluctuations in phase-separated lipid membranes by polypeptide insertion. *Biophysical Journal* **2002**, *83*, 334.
92. Ketchum, R. R.; Lee, K.-C.; Huo, S.; Cross, T. A. Macromolecular structural elucidation with solid-state NMR-derived orientational constraints. *Journal of Biomolecular NMR* **1996**, *8*, 1.

93. Kandt, C.; Ash, W. L.; Tieleman, D. P. Setting up and running molecular dynamics simulations of membrane proteins. *Methods* **2007**, *41*, 475.
94. Tian, A.; Baumgart, T. Sorting of lipids and proteins in membrane curvature gradients. *Biophysical Journal* **2009**, *96*, 2676.
95. Parthasarathy, R.; Yu, C. H.; Groves, J. T. Curvature-modulated phase separation in lipid bilayer membranes. *Langmuir* **2006**, *22*, 5095.
96. Mouritsen, O. G.; Biltonen, R.L. Protein-lipid interactions and membrane heterogeneity. *New Comprehensive Biochemistry Volume 25, Chapter 1*. Elsevier Science Publishers B.V., **1993**.
97. Yin, F.; Kindt, J.T. Atomistic simulation of hydrophobic matching effects on lipid composition near a helical peptide embedded in mixed-lipid bilayers. *Journal of Physical Chemistry B* **2010**, *114*, 8076.
98. Pautsch, A.; Schulz, G.E. Structure of the outer membrane protein A transmembrane domain. *Nature Structural & Molecular Biology* **1998**, *5* 1013.
99. Schulz G.E. Porins: general to specific, native to engineered passive pores. *Current Opinion in Structural Biology* **1996**, *6*, 485.
100. Hess, B.; Kutzner, C.; van der Spoel, D.; Lindahl, E. GROMACS 4: Algorithms for Highly Efficient, Load-Balanced, and Scalable Molecular Simulation. *Journal of Chemical Theory and Computation* **2008**, *4*, 435.
101. Marrink, S. J.; de Vries, A. H.; Mark, A. E. Coarse grained model for semiquantitative lipid simulations. *Journal of Physical Chemistry B* **2004**, *108*, 750.

102. Marrink, S. J.; Risselada, J.; Yefimov, S.; Tieleman, D. P.; de Vries, A. H. The MARTINI forcefield: coarse grained model for biomolecular simulations. *Journal of Physical Chemistry B* **2007**, *111*, 7812.
103. Monticelli, L.; Kandasamy, S. K.; Periole, X.; Larson, R.G.; Tieleman, D. P.; et al. The MARTINI coarse grained force field: extension to proteins. *Journal of Chemical Theory and Computation* **2008**, *4*, 819.
104. Periole, X.; Cavalli, M.; Marrink, S.J.; Ceruso, M. Combining an elastic network with a coarse-grained molecular force field: structure, dynamics and intermolecular recognition. *Journal of Chemical Theory and Computation* **2009**, *5*, 2531.
105. Rzepiela, A.J.; Schäfer, L.V.; Goga, N.; Risselada, H.J.; De Vries, A.H.; Marrink, S.J. Reconstruction of atomistic details from coarse-grained structures. *Journal of Computational Chemistry* **2010**, *31*, 1333.